JMB

What is the Average Conformation of Bacteriophage T4 Lysozyme in Solution? A Domain Orientation Study Using Dipolar Couplings Measured by Solution NMR

Natalie K. Goto[1,2], Nikolai R. Skrynnikov[3], Frederick W. Dahlquist[4] and Lewis E. Kay[1,3]*

[1]*Department of Biochemistry, University of Toronto, 1 King's College Circle, Toronto Ontario, M5S 1A8, Canada*

[2]*Structural Biology and Biochemistry, The Hospital for Sick Children, 555 University Ave., Toronto, Ontario M5G 1X8, Canada*

[3]*Protein Engineering Network Centers of Excellence and Departments of Molecular and Medical Genetics, and Chemistry, University of Toronto, 1 King's College Circle, Toronto, Ontario, M5S 1A8, Canada*

[4]*Institute of Molecular Biology & Department of Chemistry University of Oregon, Eugene OR 97403, USA*

Lysozyme from T4 bacteriophage is comprised of two domains that are both involved in binding substrate. Although wild-type lysozyme has been exclusively crystallized in a closed form that is similar to the peptidoglycan-bound conformation, a more open structure is thought to be required for ligand binding. To determine the relative arrangement of domains within T4 lysozyme in the solution state, dipolar couplings were measured in several different dilute liquid crystalline media by solution NMR methods. The dipolar coupling data were analyzed with a domain orientation procedure described previously that utilizes high-resolution X-ray structures. The cleft between the domains is significantly larger in the average solution structure than what is observed in the X-ray structure of the ligand-free form of the protein ($\sim 17°$ closure from solution to X-ray structures). A comparison of the solution domain orientation with X-ray-derived structures in the protein data base shows that the solution structure resembles a crystal structure obtained for the M6I mutant. Dipolar couplings were also measured on the lysozyme mutant T21C/T142C, which was oxidized to form an inter-domain disulfide bond (T4SS). In this case, the inter-domain solution structure was found to be more closed than was observed in the crystal ($\sim 11°$). Direct refinement of lysozyme crystal structures with the measured dipolar couplings using the program CNS, establishes that this degree of closure can be accommodated whilst maintaining the inter-domain cystine bond. The differences between the average solution conformations obtained using dipolar couplings and the crystal conformations for both forms of lysozyme investigated in this study illustrate the impact that crystal packing interactions can have on the arrangement of domains within proteins and the importance of alternative methods to X-ray crystallography for evaluating inter-domain structure.

© 2001 Academic Press

Keywords: T4 lysozyme; domain orientation; dipolar couplings; NMR

**Corresponding author*

Introduction

Bacteriophage T4 lysozyme is an endomuramidase utilized by the phage at a late stage in the infection cycle of *Escherichia coli* to break down the peptidoglycan walls of host bacteria.[1] This enzyme hydrolyzes the $\beta(1 \rightarrow 4)$ glycosidic linkage between the alternating units of *N*-acetylmuramic acid and N-acetylglucosamine in the peptidoglycan substrate.[2,3] X-ray crystallography has shown that T4 lysozyme has two domains, which are both involved in ligand binding.[4] The sugar moiety of the peptidoglycan substrate binds in the cleft formed between the two domains, while the peptide portion interacts exclusively with the C-terminal domain. Residues involved in catalysis, such as Glu11, Asp20, and Thr26[4-7] are all found in the

---

N-terminal domain, which is proximal to the substrate.

In the absence of ligand, wild-type (WT) T4 lysozyme crystallizes in a closed conformation resembling the structure of the peptidoglycan-bound form.[8] Initial characterization of this lysozyme crystal structure[9] led to the suggestion that entry of the relatively large substrate into the interdomain binding cleft requires a conformation that is substantially more open than that observed in the crystal. Hence, a domain-opening event should precede ligand binding if lysozyme is predominantly closed in solution. Alternatively, the X-ray structure of the wild-type enzyme may not accurately represent the average structure that exists in solution. Experimental evidence for differences between solution and crystalline forms of ligand-free lysozyme was first provided by diffuse X-ray diffraction measurements that showed that T4 lysozyme in solution is not as compact as the corresponding crystal structure.[10] Subsequently, spin-labeling studies in solution demonstrated that relative to the closed, substrate-bound conformation, T4 lysozyme exists in a more open form when substrate is not present.[11]

Insight into the potential range of conformations of T4 lysozyme in solution has been provided by X-ray crystallographic studies of lysozyme mutants.[12] In general, those mutants forming crystals that are isomorphous to the wild-type crystal (i.e. trigonal) consistently yield a closed, WT-like conformation. Conversely, different crystal forms trap conformations distinct from this wild-type closed structure. A directed effort to procure a variety of lysozyme crystal forms produced a library of structures with different relative domain orientations.[12] Some mutants are very open relative to the wild-type form, whilst others are more closed, with the group of mutants spanning a 50° range of hinge-bending angles. In addition, lysozyme mutants such as M6I and I3P crystallized with more than one protein molecule in the asymmetric unit, each with a different conformation.[13,14] These mutants could also be crystallized in a form isomorphous to the WT crystals, resulting in structures with the WT closed conformation. Hence, the various mutations probably do not change the conformational properties of lysozyme in solution, but instead alter the type of packing interactions that can occur between proteins in the crystal.

Based on the conformational variability displayed by the different lysozyme mutants, it appears that in the absence of substrate, lysozyme may be able to access a wide range of conformations in solution. However, the relative population of each conformation and hence the average solution conformation of T4 lysozyme is not known. Solution NMR studies have established that the secondary structure and intra-domain fold of lysozyme are similar to that of the crystalline form,[15,16] yet the precise arrangement of domains within the protein has not been determined in the liquid-state. In spite of this gap in our knowledge,

T4 lysozyme has been extensively utilized as a model protein system to study protein folding,[17,18] glycosidase activity[4,19] and the effects of cavity-creating mutations within a protein hydrophobic core.[20,21] This protein has also served as a reliable standard for the development of methods in protein crystallization,[22,23] NMR spectroscopy,[24,25] molecular dynamics simulations[26,27] and spin labeling.[11,28,48] Consequently, a complete description of the structure of T4 lysozyme that includes the relative orientation of domains in an aqueous environment will benefit our understanding of the protein itself, and can be useful in the interpretation of results from experiments using lysozyme as the model system.

The question of relative domain orientation in the liquid state requires the measurement of global restraints that can give information on protein fragments that may be far apart in space. It has been shown that dipolar couplings measured in weakly aligning media can be used to obtain this type of long-range orientational information.[29–36] A number of applications involving the use of dipolar couplings in structural studies of protein complexes or multi-domain proteins have appeared recently.[36-40] When one or more high-resolution structures are available for the domains of a multi-domain protein, then a straightforward method of determining domain orientation can be used that fits the measured dipolar couplings to those predicted from a protein structure on a per-domain basis.[29,37]

In this work, ^1HN-^{15}N dipolar couplings are used to address the question of T4 lysozyme conformation in solution. Dipolar couplings have been measured in several different aligning media and the accuracy of domain orientation procedures evaluated in cases where a limited number of dipolar couplings are available, considering the uncertainty typically associated with high-resolution X-ray structures. Using this protocol, we find that, unlike the crystal form, wild-type lysozyme in solution exists in an open conformation resembling that of the M6I mutant. Similarly, a lysozyme mutant forced into a closed conformation *via* an inter-domain disulfide bond also shows differences with the corresponding crystal structure. In this case, the structure is more closed in solution than in the crystal form. The discrepancies observed between liquid and crystal-state conformations of T4 lysozyme highlight the potential differences that can occur between X-ray and solution conformations of proteins involving structural features that arise from weak interactions.

Results and Discussion

Data used in orientation analyses

In this study, ^{15}N-^1HN residual dipolar couplings were measured on ^{15}N or ^{15}N,^{13}C-labeled samples of C54T/C97A (WT*) T4 lysozyme (Figure 1), which has been shown to have WT
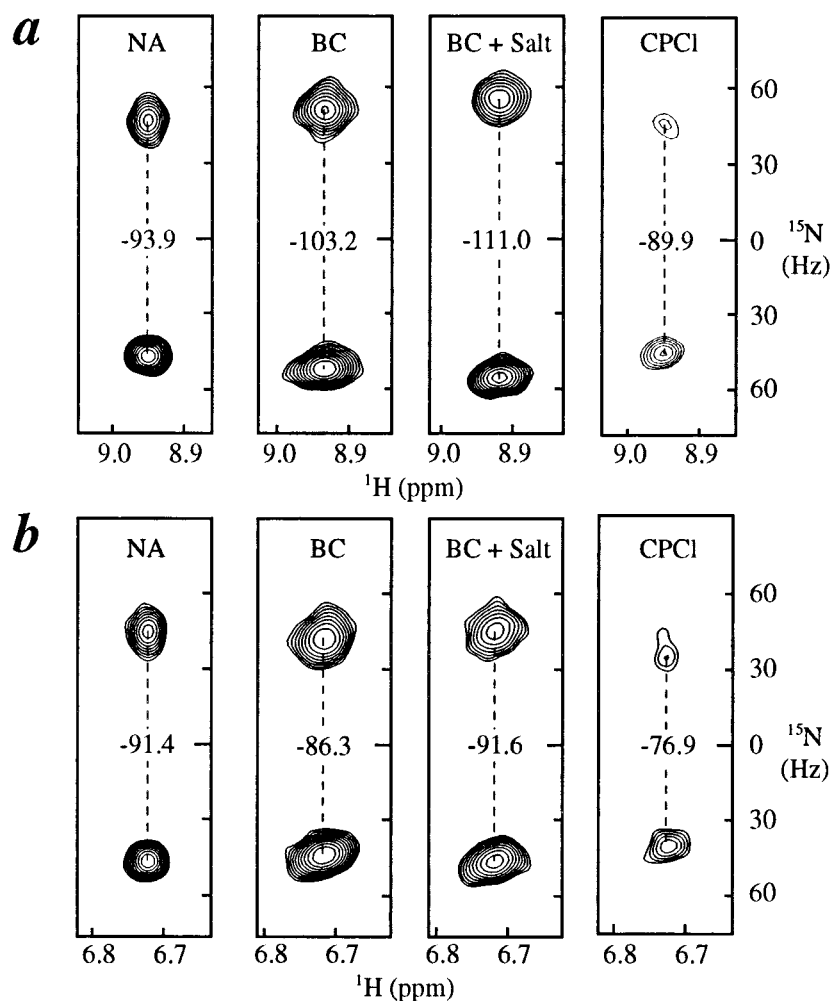
Figure 1. Selected regions of ^{15}N-[1]HN IPAP-HSQC spectra for T4SS in the indicated alignment media for residues (a) Leu39 and (b) Trp126 (where spectra containing upfield and downfield peaks have been superimposed). NA refers to the sample that is not aligned, while brief descriptions of the aligned samples are given in Table 1. The zero point on the vertical scale is centered between the two peaks in the doublet and measured splittings are given for each doublet in Hz. Low peak intensities in the CPCl spectra arise from the low concentration of protein for this particular sample (0.2 mM, as described in Materials and Methods).

structure and activity.[41] Dipolar couplings for WT* have been recorded in four different aligning solvents, three of which were bicelle media[42] and the other a lamellar phase produced by cetylpyridinium chloride (CPCl) with hexanol.[43,44] Two different concentrations of bicelles were used (which we refer to as high BC and BC) with another BC sample also comprised of 150 mM salt (BC + salt). The average number of dipolar couplings measured on ^{15}N-labeled WT* lysozyme in each bicelle medium (Table 1) is 26 ± 2 and 34 ± 4 for the N and C-domains, respectively. In the case where ^{15}N,[13]C-labeled protein was available (WT*, CPCl; see Table 1), a 3D HNCO-based experiment was used to measure dipolar couplings, as described in the legend to Figure 8. Approximately twice as many dipolar couplings were measured in this case, due to the reduction in peak overlap relative to 2D IPAP experiments.[45,46] Dipolar couplings were measured for ^{15}N-labeled T4SS in bicelles with or without salt as well as in CPCl liquid crystals. Fewer dipolar couplings were obtained for T4SS relative to WT*, since overlap of peaks in 2D [15]N-[1]HN spectra was more pronounced for the disulfide mutant.

Because the largest source of variability in using dipolar couplings to obtain the relative orientation of domains is the uncertainty in intradomain structure of the starting X-ray or NMR derived structures,[29] nine different X-ray starting structures were used in the analysis (Table 2). Note that the structure of T4SS and the PDB coordinates 150L(c) were not used in the analysis. The resolution of these structures is 2.0 Å or better and the list includes conformations that are both more closed and more open than the WT crystal structure. The intradomain pairwise rmsd between backbone heavy atoms in the structures is 0.1-0.5 Å for the C-domain (residues 1-10 and 81-160) and 0.1-0.6 Å for the N-domain (residues 13-65). So that all structures and subsequent analyses could be described with respect to a common molecular frame, the C-domain of each structure was superimposed onto the WT (3LZM) C-domain. The relative domain orientation of each structure could then be described with respect to the WT conformation using the rotations required to superimpose the N-domain of WT lysozyme onto the N-domain of the indicated structure. Each of these transformations is listed in Table 2 in terms of rotations

Table 1. Summary of dipolar coupling data used in domain orientation analyses

			$^2H^a \, \Delta v$			Number of DCs[c]	
Sample		Alignment medium	(Hz)	$A_a^b \times 10^{-3}$	R	C	N
WT*	High BC	7.5% (w/v) bicelles	14.1	2.48	0.215	29	23
	BC	5% (w/v) bicelles	8.9	1.46	0.198	38	28
	BC+salt	5% (w/v) bicelles, 150 mM NaCl	8.6	1.49	0.194	35	27
	CPCl	CPCl/hexanol, 200 mM NaCl	5.5	0.59	0.131	83	50
T4SS	BC	5% (w/v) bicelles	8.9	1.24	0.151	32	28
	BC+salt	5% (w/v) bicelles, 150 mM NaCl	8.7	1.36	0.244	31	28
	CPCl	CPCl/hexanol, 200 mM NaCl	7.3	−0.80	0.663	27	22

[a] Quadrupole splitting (^2H_2O).
[b] Alignment parameters A_a and R (equation (2)) were determined using the 3LZM crystal structure with dipolar couplings from the indicated alignment medium. Preceding this calculation, the relative domain orientation of 3LZM was altered to reflect the solution conformation as determined using this structure and the dipolar coupling data.
[c] The number of dipolar couplings measured on the C-domain (C) or N-domain (N).

about the closure, bend and twist axes, as outlined in Materials and Methods. Rotations about this same axis system were used to describe the relationship between a reference structure (X-ray structures of WT* and T4SS were used as references in the analysis of WT* and T4SS data, respectively) and the solution state conformations derived from the dipolar couplings. A detailed description of the methodology used in the analysis of the dipolar coupling data in terms of relative domain orientation is provided in Materials and Methods and the results of the analysis are described in what follows.

Relative domain orientation of WT* T4 lysozyme

Results from the domain orientation procedure described in Materials and Methods for the family of input crystal structures listed in Table 1 using

dipolar couplings measured on WT* lysozyme are summarized in Figure 2, with each of the plots, (a)-(d), corresponding to data recorded in different aligning media. The transformations required to overlay the N-domain of the WT X-ray structure (3LZM) on the corresponding N-domains of each of the X-ray structures used in the analysis (C-domains of all structures are aligned) are given by open dots in the Figure. In addition, the transformations of the N-domains of each of the X-ray structures required to produce structures that best satisfy the experimental dipolar couplings are indicated by filled dots. In the approach taken here (see Materials and Methods), the individual N and C-domains of each X-ray structure are first superimposed on the corresponding domains of the reference structure, 3LZM, and the dipolar coupling data used to reorient each N-domain. The transformation from the reference structure to the corresponding solution structure or to another

Table 2. Summary of T4 lysozyme X-ray crystal structures used in analyses

PDB I.D.[a]	Mutation	Closure[b]	Bend[b]	Twist[b]
152L	3SS[c]	8°	5°	2°
TBA[d]	T4SS[e]	4°	3°	0°
148L	T26E[f]	3°	1°	4°
3LZM	WT	0°	0°	0°
1LYD	WT	0°	0°	0°
1L90	L99A	0°	−1°	0°
137L(a)	S44F (WT*[g])	−3°	4°	0°
137L(b)	S44F (WT*[g])	−8°	−2°	−7°
150L(c)[d,h]	M6I	−18°	3°	−18°
173L	"Quad"[i]	−29°	−6°	−25°
172L	I3C	−37°	−4°	−13°

[a] 3LZM;[72] 1LYD;[96] 1L90;[92,93] 137L;[94] 148L;[6] 152L;[95] 172L and 173L;[12] 150L(c);[13] TBA.[49]
[b] Closure, bend and twist rotations required to superimpose the N-domain of 3LZM onto the N-domain of the indicated structure. More open structures have negative closure and twist.
[c] Triple mutant I9C/L164C, T21C/T142C and I3C/C97 resulting in disulfides at 9-164, 21-142 and 3-97.
[d] Not used as an input structure in domain orientation analyses. PDB accession code not available for T4SS.
[e] T21C/T142C (WT* background), oxidized to form interdomain disulfide bond. This structure was used as the reference structure in the analysis of all T4SS dipolar couplings.
[f] Covalently modified by peptidoglycan substrate.
[g] C54T/C97A.
[h] M6I structure C of four distinct structures in the asymmetric unit labeled A-D.
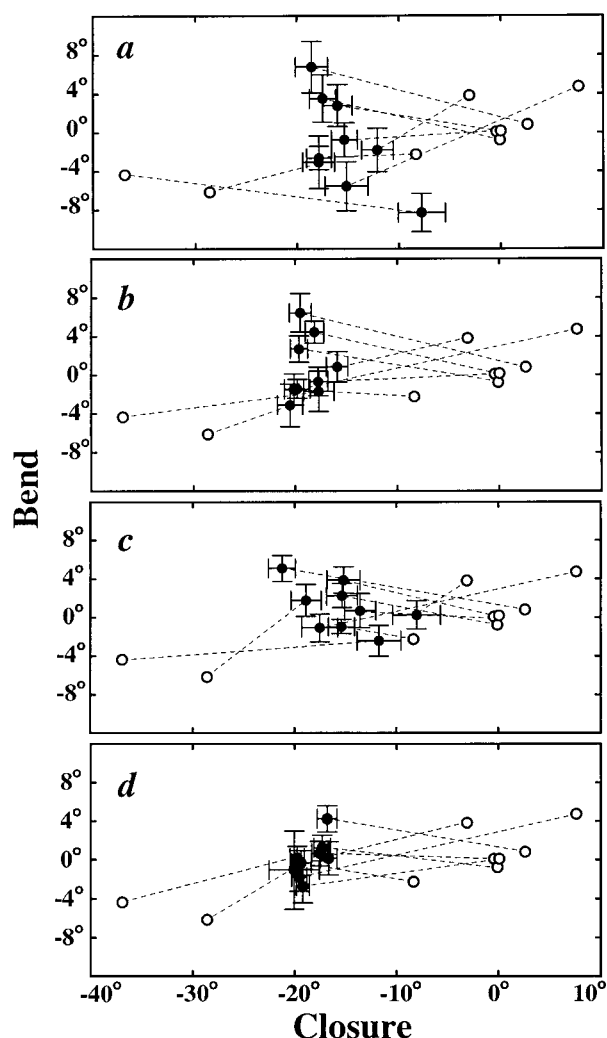[i] K16E/K119E/R135E/K147E.

Figure 2. Relative domain orientations obtained from dipolar couplings measured on WT* lysozyme in (a) 7.5 % (w/v) bicelles, (b) 5 % bicelles, (c) 5 % bicelles, 150 mM NaCl or (d) CPCl/hexanol, 200 mM NaCl. Plotted are closure and bend rotations that transform the WT structure into either a starting X-ray structure (open circles) or a solution conformation consistent with the dipolar couplings (filled circles). Negative closure and bend values indicate structures that are more open with respect to the WT crystal structure (3LZM). Broken lines connect each starting X-ray structure with the counterpart solution conformation determined using dipolar couplings. Error bars associated with each solution conformation were obtained using a jackknife procedure as described in Materials and Methods.

X-ray structure is described in terms of rotations about an axis system comprised of closure, twist and bend axes, illustrated in Figure 3 and described in detail in Materials and Methods. Since the precision in the twist dimension is often poor (see below), only closure and bend are represented in these plots. Broken lines connect the solution structures indicated by the filled dots with the initial X-ray structures that were used as input.

In the analyses of WT* data, the closed WT crystal structure (3LZM) was used as the reference conformation. Consequently, if the average relative domain orientation of WT* in solution is represented accurately by this X-ray structure, then the closure, bend and twist angles obtained from the domain orientation procedure would be {0°, 0°, 0°}. In contrast, the graphs show that the solution conformation is more open than this closed X-ray structure, with values that lie within the range of −8° to −22° for closure. Bend values scatter evenly around 0° with a range as large as ±8°. Rotations in the twist dimension (data not shown) have even larger scatter with a range from −13° to 32°. The variability associated with errors in the dipolar coupling measurements (given by the error bars) was less than ±2° for closure and bend, and typically of the order of ±5° for twist (see Materials and Methods for details of calculations).

The average solution conformation determined in each aligning medium can be represented by the average closure, bend and twist angles calculated over the group of solutions obtained from the nine different input structures (Table 3). Closure values of −15° to −19° were obtained from the different media (Table 1), suggesting an average solution conformation that is significantly more open compared to the WT X-ray crystal structure. The range of twist rotations obtained from the various aligning media is −7° to −18°, similar to some of the twist values required to transform 3LZM to a number of open crystal structures (Table 2). Hence, the average conformation of WT* in solution is more open in both the closure and twist dimensions than the 3LZM X-ray structure. This relative domain orientation is an intrinsic feature of native lysozyme, since dipolar couplings measured on the wild-type protein in CPCl give results that agree closely with those for WT* (data not shown).

The errors reported in Table 3 correspond to the variation in closure, twist and bend angles that

Table 3. Mean closure bend and twist (in degrees)

Sample		Closure	Bend	Twist
WT*[a]				
	High BC	−15 ± 4	−1 ± 5	−15 ± 11
	BC	−19 ± 2	1 ± 3	−16 ± 10
	BC+salt	−15 ± 4	1 ± 3	−18 ± 8
	CPCl	−18 ± 2	0 ± 2	−7 ± 11
T4SS[b]				
	BC	11 ± 3	1 ± 4	14 ± 12
	BC+salt	9 ± 4	1 ± 3	−5 ± 17
	CPCl	12 ± 4	−1 ± 5	1 ± 6

[a] All results for WT* lysozyme are reported with respect to the WT X-ray crystal structure (3LZM). Negative values correspond to more open solution conformations relative to this reference structure.
[b] The X-ray crystal structure for T4SS (T21C/T142C) lysozyme has been used as the reference structure in the determination of closure, bend and twist. Positive values indicate a solution conformation that is more closed than the reference X-ray crystal structure.
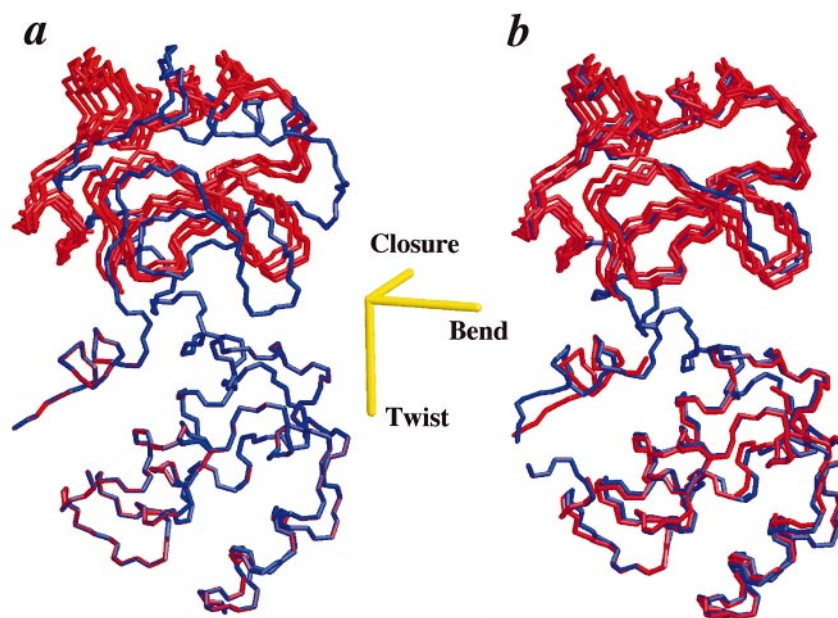
Figure 3. Solution conformations of WT* lysozyme as determined from dipolar couplings (in red) where the C-domain is superimposed onto either (a) the WT X-ray structure (3LZM) or (b) the X-ray structure of the M6I mutant (150L(c)). Solution conformations obtained from dipolar couplings recorded in each of the four aligning media (Table 1) were reconstructed using the domain structure from the WT (3LZM) crystal structure with the rotations given in Table 3. Linking hinge regions were not included in the reconstruction of solution conformations. The axes of closure, bend and twist are shown in the same molecular frame for reference. Details regarding the reconstruction of solution conformations are given in Materials and Methods.

arises from differences in domain structure within the group of lysozyme crystal structures used in this analysis (given by the scatter of the filled dots in Figure 2). In general, this intradomain structural noise gives rise to variations of about $\pm 2^\circ$- $\pm 5^\circ$ in both closure and bend. In the twist dimension a larger error of $\pm 8^\circ$- $\pm 11^\circ$ is obtained. As discussed below, the impact of small differences in intradomain structure also depends on the rhombicity of the alignment, as well as the alignment tensor orientation with respect to the closure, bend and twist axes.

Solution conformations of WT* lysozyme were reconstructed from the N and C-domains of the 3LZM crystal structure using the rotation parameters in Table 3, along with the positional information obtained from pairs of crystal structures as described in Materials and Methods. Figure 3 shows four models of the solution conformation of WT* lysozyme (red) based on the dipolar coupling data recorded in the four different aligning media. Each of the solution structures is reconstructed starting from the 3LZM coordinates. Reasonable agreement among models based on data from different alignment media is established by the distance rmsd between pairs of reconstructed structures, which range from 0.7-2.6 Å for backbone atoms. For the sake of comparison, X-ray structures (blue) are shown for either (a) WT (3LZM) or (b) the M6I mutant (150L(c)) with the C-domains of each structure superimposed on the C-domains of the solution structures (the 3LZM C-domain). It is

clear from this reconstruction that whilst the solution conformation of WT* lysozyme differs from the crystal structure of WT, there is good agreement with the open M6I crystal form. The backbone rmsd values between N-domains from M6I and each reconstructed solution conformation vary from 0.7-2.9 Å (note that perfect agreement in domain orientation would still give rise to 0.36 Å rmsd between 150L(c) and solution N-domains due to structural noise). Previous studies using site-directed, spin-labeled, ligand-free lysozyme[11,47] are consistent with these results. In these experiments, the distance separating a pair of spin-labels was estimated from the broadening in electron paramagnetic resonance (EPR) spectra and found to agree well with predictions based on structural models of spin-labeled 150L(c).

Relative domain orientation of T4SS

The results from the domain orientation analyses on WT* lysozyme suggest that crystal packing forces lead to a structure in the crystal state that is quite different from the open conformation that exists in solution. It is of considerable interest to compare X-ray and solution structures of a more constrained molecule, which might be less sensitive to the effects of such packing interactions. With this in mind, we have determined the relative domain orientation of a conformationally restricted form of T4 lysozyme, generated by the double mutation T21C/T142C, (WT* background) under

oxidizing conditions.[49] The activity of this lysozyme mutant (T4SS) can be controlled by the redox potential of the aqueous environment, since it is active only when reduced.[41] X-ray crystallography of oxidized T4SS shows that there is a disulfide bond linking the two domains across the binding cleft, leading to a structure that is slightly more closed than WT (Table 2). In fact, the observed degree of domain closure is necessary for disulfide-bond formation, since the distance separating the Cys C$^\alpha$ atoms in the structure of the reduced form of the protein (8.1 Å) is outside the range normally observed for cystine bonds in proteins (4.6 Å-7.4 Å).[50] This covalent interdomain association prevents T4SS from forming structures that are more open than WT.

The relative domain orientation of T4SS was evaluated using the same procedure as described for WT*, except that closure, bend and twist angles describe the transformations from the crystal structure of T4SS instead of WT to the solution conformations. Figure 4 summarizes the closure and bend obtained in the three different aligning media (Table 1). The solution domain orientations give rise to structures that are more closed than the T4SS crystal structure by 2°-18°. Similar to the WT* analysis, bend values are roughly distributed
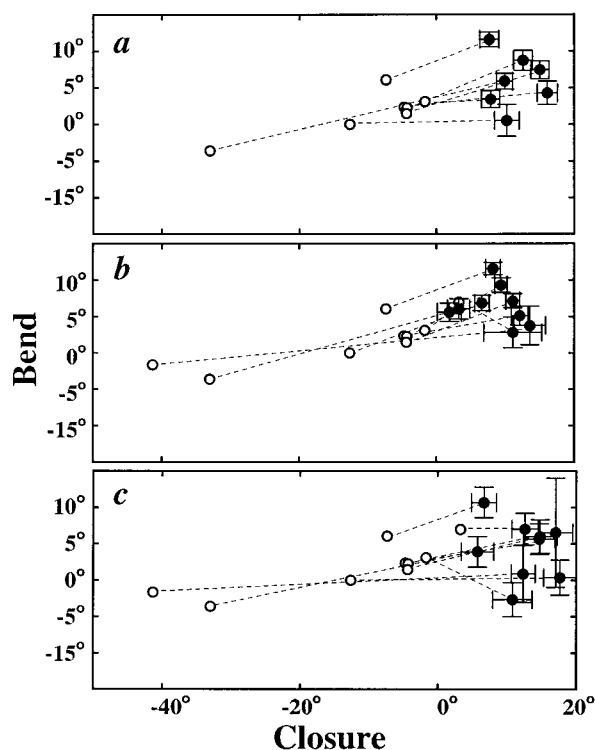
around 0° with a range of ±7°. The average relative domain orientations calculated for each medium are shown in the bottom half of Table 3. In all cases, solution conformations are obtained that are more closed than what is observed in the T4SS crystal structure. There is significant variation in twist values, reflecting the uncertainty in this parameter (see below). Although the rhombicity of the alignment tensor was low in the bicelle media, a high rhombicity value was obtained in CPCl (Table 1), leading to reduced error in the twist dimension in this case (see below). Hence the twist of 1° obtained in this medium represents the twist of the solution conformation relative to T4SS more accurately.

T4SS solution conformations were reconstructed using the rotation parameters obtained from the analyses described above (Table 3) and the same pivot position used to generate the WT* solution conformations (see Materials and Methods). Reconstructed solution conformations with C-domains superimposed on the C-domain of the T4SS crystal structure are shown in Figure 5(a). As shown by this representation, the dipolar couplings are consistent with structures that are more closed than the X-ray structure. Even when compared to the crystal structure of the most closed conformation in the lysozyme database, 152L (with three interdomain disulfide bonds), Figure 5(b), closure is still more pronounced in solution. The agreement between conformations obtained in different media is not as high as realized for the WT data, with pairwise rmsd values ranging from 1.5 Å-4.1 Å. These differences largely reflect variation in the twist results as discussed above. In addition, in these reconstructions the Cys C$^\alpha$ separation distance is between 2.9 and 4.4 Å, which is not within the favored range for disulfide-bond formation (4.6-7.4 Å).[50] However, the relative position of domains depends critically on positional parameters adopted in the rigid-body transformation used in the reconstruction (pivot and translation in Equation (4), described in Materials and Methods). These parameters are not available from dipolar coupling measurements and are not known to great accuracy. With a 0.2 to −2.5 Å translation (depending on which of the three solutions is considered), it is possible to rectify the Cys C$^\alpha$ separation distance. Physically reasonable models of T4SS with the relative domain orientation established by the dipolar couplings can be built using direct refinement protocols, as described in the next section.

Figure 4. Relative domain orientation obtained from dipolar couplings measured on T4SS in (a) 5% bicelles, (b) 5% bicelles, 150 mM NaCl or (c) CPCl/hexanol, 200 mM NaCl. Rotations are described with respect to the reference X-ray crystal structure of T4SS. Results from structures 152L and 172L in (a) were not included, since large Ω values were obtained (see Materials and Methods).

Relative domain positioning

Although it has been possible to use dipolar couplings to obtain the relative orientation of domains and hence the degree of domain closure, information on the relative positions of domains is not obtained by this method. As shown for T4SS, this can lead to uncertainty in the reconstruction of solution conformations. However, the existing
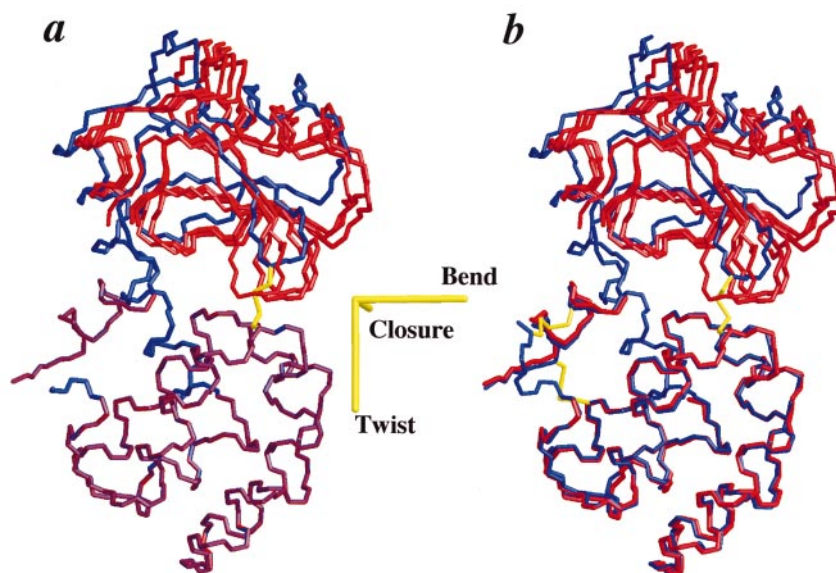
Figure 5. Solution conformations of T4SS lysozyme obtained from the dipolar couplings in each aligning medium (red structures) where the C-domain is superimposed on the C-domain of the crystal structure of (a) T4SS or (b) the C-domain of the structure of the most closed conformer available (152L). Disulfide linkages in the crystal structures are shown in yellow.

database of lysozyme crystal structures with a wide range of hinge-bending angles provides an opportunity to identify structures that give reasonable fits to the measured dipolar couplings. The quality of the fit between the experimental dipolar couplings (D^{meas}) and those calculated based on starting X-ray structures was evaluated using the quality factor, Q:[46]

$$Q = \sqrt{\frac{\sum_{i=1,N}(D_i^{meas} - D_i^{calc})^2}{\sum_{i=1,N}(D_i^{meas})^2}} \qquad (1)$$

with D_i^{calc} calculated as described in Materials and Methods. Defined in this way, the quality factor is sensitive to interdomain structure (i.e. the relative orientation of domains) as well as to small differences between the structures of each of the domains in the solution and X-ray states (intradomain structure). In order to minimize the contribution of intradomain structural differences in this comparison, the Q-factors (columns 3 and 4 of Table 4) were normalized by the Q-factor obtained after domain alignment using the dipolar couplings. These Q-factors, indicated under the column titled Norm in Table 4, contain contributions from intradomain structural differences only. Hence the normalized Q-values (Q/Norm) indicate how well the interdomain structure described by a given set of X-ray coordinates reflects the solution conformation. As shown in Table 4, the best agreement between dipolar couplings collected on WT* and those predicted from an X-ray structure is obtained for the open conformation of lysozyme given by the mutant M6I (150L(c)) that is shown in Figure 3(b). Structures that are more open (172L) or more closed (3LZM) produced poorer fits to the experimental dipolar couplings. In the case of

T4SS, experimental dipolar couplings fit best to those calculated using the most closed conformation in the database, 152L. These crystal structures can thus be considered to represent physically reasonable models for the average solution conformation.

It is also possible to directly evaluate whether a given crystal structure with its relative domain positioning and linker conformation is consistent with experimental dipolar couplings by prediction of alignment tensor parameters based on the molecular shape of the protein. When dipolar couplings are measured in a medium that induces alignment through a purely steric mechanism alignment tensor parameters can be predicted.[51] Since the alignment tensor prediction is based on the shape of the molecule, this method is sensitive to the displacement between the two domains as well as to the structure of the intervening linker regions.

Using the program SSIA (simulation of sterically induced alignment),[51] we compared dipolar couplings calculated from the predicted alignment tensor with those measured using the bicelle sample with salt, since this medium is the least likely to have electrostatic contributions to alignment. Table 4 shows that the normalized Q-factor calculated between SSIA-predicted and experimental dipolar couplings is lowest when the M6I (150L(c)) structure is used. When structures that are either more open (172L) or more closed (3LZM) than 150L(c) are used to predict the alignment tensor, the normalized Q-factor increases. Of interest, the agreement between the SSIA-predicted and the experimental dipolar couplings for the M6I structure is comparable to that obtained with the dipolar couplings and those predicted based on fits of the couplings to the X-ray structure (SVD). The SSIA analysis indicates that the linker structure and relative domain arrangement in the M6I open

Table 4. Comparison of measured dipolar couplings with those predicted from the sterically induced model of alignment

Sample[a]	Crystal structure[b]	Q-factor:			Normalized Q[f]	
		SVD[c]	SSIA[d]	Norm[e]	SVD	SSIA
WT*	150L(c)	0.31	0.32	0.29	1.1	1.1
	172L	0.41	0.55	0.31	1.3	1.8
	3LZM	0.34	0.48	0.26	1.3	1.8
T4SS	152L	0.25	0.27	0.23	1.1	1.2
	TBA[g]	0.25	0.36	0.21	1.2	1.7
	150L(c)	0.58	0.70	0.23	2.5	3.0

[a] Dipolar coupling data set measured in 5 % (w/v) bicelles, 150 mM NaCl with the indicated lysozyme sample.
[b] PDB identifier of the X-ray structure used in the analysis (SVD) or prediction (SSIA) of dipolar couplings.
[c] The quality (Q) factor (equation (1)) calculated according to Ottiger & Bax[97] obtained from singular value decomposition (SVD) using the measured dipolar couplings and the indicated structure.[56] Domains in the structure have not been oriented.
[d] The Q-factor comparing the agreement between experimental dipolar couplings and those predicted using the 5 % (w/v) bicelle model in SSIA.[51]
[e] Domains of the indicated crystal structure are re-oriented using the experimental dipolar couplings. Subsequently Q-factors are calculated and reported as Norm.
[f] Q-factors (SVD) normalized by the domain orientation independent Q-factor (Norm) for the indicated structure.
[g] TBA refers to the X-ray coordinates of T4SS, which are in the processes of being submitted to the PDB.

structure is consistent with the experimental dipolar couplings.

A similar analysis of the T4SS solution conformation shows that the best fit to the measured set of dipolar couplings is obtained using the SSIA-predicted dipolar couplings from 152L, which is the most closed lysozyme structure in the PDB. Consequently, of the available X-ray crystal structures, 152L most accurately represents the average solution conformation of T4SS. However, the extent of domain closure in 152L is still less than that obtained from the dipolar couplings.

Finally, it is noteworthy that the SSIA analysis predicts similar degrees of alignment for both open (172L, 173L) and closed (3LZM) conformations of lysozyme. Thus the dipolar couplings measured reflect the conformational preferences of the whole population of molecules in solution and not simply a subset that might orient far better than the rest, for example.

As noted in the previous section, inaccurate estimates of positional parameters required to reconstruct a solution conformation for T4SS (Figure 5), result in structures where the disulfide C^α atoms are too close. Physically reasonable models of the solution conformation of T4SS can be produced with a relative domain orientation that agrees with the measured dipolar couplings using a rigid-body refinement protocol in the structure calculation program CNS.[52] In this procedure (described in Materials and Methods), T4SS solution structures were generated starting from the parent crystal structure or from 3LZM, with T21 and T142 replaced with Cys. Low-temperature torsion angle simulated annealing was performed using an experimental set of dipolar couplings and tight intradomain structural restraints generated from the crystal structures to preserve the domain structure. The results from this refinement procedure are shown in Figure 6, in red, superimposed onto the crystal structure of T4SS, in blue. It is clear that

the T4SS structure in solution is more closed than in the crystal. The average closure, bend and twist angles of {10°, 2°, 2°} that describe the domain orientation of these structures relative to the T4SS reference structure agree well with values obtained from the domain orientation protocol shown in Table 3. As expected, disulfide-bond formation is now accommodated by these structures, with Cys 21/Cys 142 C^α separation distances of 4.8 Å-5.5 Å.

Of the more than 300 available X-ray crystal structures of wild-type and mutant T4 lysozyme in the PDB, more than 90 % occur in a crystal form that leads to the closed conformation. These crystals arise from the formation of a ''back-to-back'' dimer (where the ''front'' is the substrate-binding site) that buries 800 Å^2 of surface area per molecule when in the WT closed form.[12] One example of this dimer does exist for a mutant in the open conformation; however, the amount of surface area buried by the intermolecular dimer drops by more than 50 % relative to dimers formed by closed conformations. This implies that there is a cost in crystal packing energy for this favored crystal form if the conformation of lysozyme deviates from the WT closed position. It may be that formation of this dimer by T4SS in the crystal lattice favors a structure that is slightly open relative to the very closed average conformation observed in solution in order to maximize the surface area at the dimer interface. This can be readily accommodated, since changes in disulfide bond conformations permit a range of possible relative domain arrangements at low energetic cost.[50]

Possible sources of error in domain orientation analyses

It has been shown in a number of cases that alignment induced by weak binding of single-domain proteins to the alignment media does not measurably affect the structure.[53−55] However, the
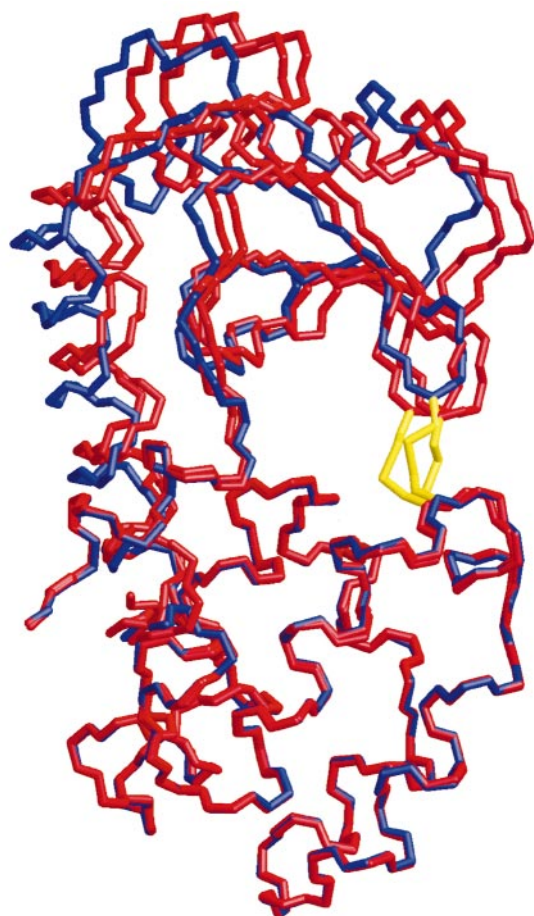
Figure 6. Models of solution conformations of T4SS (red) generated using rigid-body refinement in CNS as described in Materials and Methods, with C-domains superimposed on the crystal structure of T4SS (blue). Crystal structures of T4SS and WT (3LZM) with T21 and T142 side-chains mutated *in silico* to Cys were used as starting structures in the calculations.

energy required to change the relative arrangement of domains in a multi-domain protein may be small, leading to concerns regarding the effect of the aligning medium on the observed relative domain orientation. With this in mind, we have measured dipolar couplings using a number of different alignment media, under a variety of ionic

strength conditions. Good agreement between conformations was obtained in all bicelle media tested (Table 3). In addition, very similar relative domain orientations were obtained from dipolar couplings measured in CPCl/hexanol liquid crystals, which have very different chemical and electrostatic properties relative to bicelles. The similarity in results obtained from different aligning media gives confidence in the solution conformations estimated for WT* and T4SS.

In the present study, we found that, depending on the aligning medium used, the precision in closure and bend angles ranged between $\pm 2°$ and $\pm 5°$, whilst the precision in the twist angle was as low as $\pm 17°$ in one case (Table 3). This level of precision compares rather poorly (a precision of $1°$, $2°$ and $3°$ in the closure, bend and twist dimensions, respectively), with what we observed in a study of domain orientation in maltose-binding protein, where a very large number of dipolar couplings (~ 1400) was recorded.[29] In order to understand the factors that contribute to the precision in closure, bend and twist, a set of dipolar couplings have been calculated using the X-ray structure of WT lysozyme, 3LZM, with an experimentally determined alignment tensor (parameters given in the legend to Figure 7) that is the same for both the N and C-domains (i.e. the relative orientation of domains is described by the 3LZM structure in this analysis). Closure, twist and bend angles were then calculated using these dipolar couplings in concert with the same family of structures used to analyze the experimental data, described above. Since the simulated solution structure is the same as the reference structure (3LZM), the target closure, bend and twist angles are $\{0°, 0°, 0°\}$. As shown in Figure 7(a), when dipolar couplings are calculated with a rhombicity of 0.17 and all residues in the two domains are used (88 C and 53 N-domain residues), closure and bend are determined quite precisely. Not unexpectedly, reducing the number of couplings (simulated BC data set with 38 C and 28 N-domain couplings), leads to an increase in the sensitivity to structural noise associated with the different starting X-ray structures (see Figure 7(b) and Table 5). Lowering the rhombicity from 0.17 to 0.10 leads to a further reduction in both the accuracy and precision of the bend angle (Figure 7(c)-(d) and Table 5). It is interesting to note that in all of the examples considered here,

Table 5. Average relative domain orientations (in degrees) from simulated dipolar couplings

| | Number of DCs from each domain | | | | | |
	R	C	N	Closure	Bend	Twist
a,e	0.17	88	52	0 ± 2	0 ± 2	6 ± 10
b,e		29	23	0 ± 3	-4 ± 4	-5 ± 11
c,e	0.10	88	52	0 ± 1	1 ± 4	10 ± 17
d,e		29	23	0 ± 3	-5 ± 5	-11 ± 17

[a-d] in the Table give averages for the corresponding graphs in Figure 7.
[e] Results were calculated using simulated dipolar couplings as described in the text and in the legend to Figure 7.
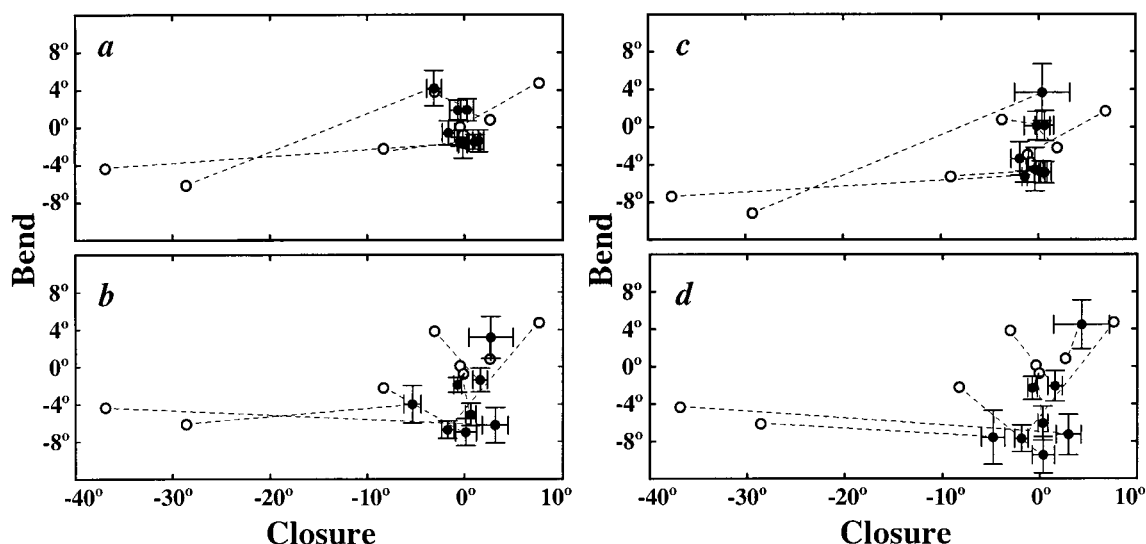
Figure 7. Domain orientation from a simulated set of dipolar couplings calculated using the WT reference structure (3LZM). Residues for which dipolar couplings were available in the CPCl WT* data set (Table 1) were used to generate the results in (a) and (c), whilst a smaller data set was used to calculate (b) and (d), including only those residues contained in the BC WT* data set. Rhombicity was set to (a) and (b) 0.17 or (c) and (d) 0.10. The alignment tensor parameters used to calculate the simulated data were $A_a = 1.5 \times 10^{-3}$, $\alpha = 186°$, $\beta = 142°$, $\gamma = 54°$ (same parameters used for both N and C-domains). Domain orientations in the form of closure and bend values were computed using these simulated dipolar couplings and the family of crystal structures listed in Table 1, as described in the text.

the accuracy in the twist dimension is poor, as is the precision. Note that the spread in closure and bend values obtained in the present simulation is similar to what is observed experimentally.

The ability to define rotations about the Z-axis of the alignment frame accurately is related to the magnitude of the rhombic component of the alignment tensor.[42,56] The Z-axis of the alignment tensor used in the simulations described above (and the axis measured experimentally) is almost coincident with the twist axis (15° between the two axes) and in concert with a low rhombicity, R, leads to poor definition of relative domain orientation with respect to twist. The precision in closure and bend is also dependent on the orientation of the Z-axis of alignment. In the simulated data sets, the projection of the Z-axis of alignment onto the bend axis is almost twofold larger than that for the closure axis (0.23 for bend *versus* 0.14 for closure). As a result, differences in intradomain structure lead to greater variability in bend compared to closure. In summary, the number of couplings, the rhombicity and orientation of the alignment tensor in conjunction with structural noise are all important factors that affect the precision and accuracy of the domain orientation procedure.

According to analyses of lysozyme open and closed crystal structures, the C-domain is comprised of the C-terminal half of the protein, as well as the N-terminal α-helix (residues 1-10, helix A). However, the identification of dynamic domains has led to the suggestion that the C-domain may not include this N-terminal α-helix.[57,58] A comparison of open and closed structures show that the

orientation of this helix does change slightly upon opening, leading to the formation of new packing interactions.[12,14] As a result, the mean pairwise rmsd between C-domains in the group of input structures is significantly higher with this helix (0.42 Å) than without it (0.27 Å). In order to determine whether structural noise arising from this helix could lead to systematic contributions to domain closure values, domain orientation analyses were performed where the N-terminal helix was removed from calculations. Closure and bend values remained to within 2° of the original angles, with twist affected to a larger degree (as large as an 8° difference) with no systematic change.

Concluding remarks

T4 lysozyme binds to its substrate through interactions over an extended surface on the C-domain with N-domain residues involved in both binding and catalysis. The domain orientation results presented above establish that in the absence of substrate native T4 lysozyme exists, in solution on average, in a conformation that is more open than that observed in the crystal state. Since entry of the relatively large peptidoglycan substrate into the binding cleft is likely facilitated by a more open conformation, it appears that lysozyme normally exists in a state primed for binding. As shown by spin-labeling studies, a covalently linked substrate-lysozyme complex strongly favors a closed conformation.[11] In the absence of a covalent link, the ability of lysozyme to successfully bind its ligand

before it has a chance to escape from the binding pocket likely requires rapid domain closure. Low energy barriers to domain motion can facilitate this transition, but may lead to a significant proportion of lysozyme existing in a closed conformation in the absence of ligand.

Examination of the range of ligand-free lysozyme structures obtained from X-ray crystallography has led to the suggestion that the equilibrium state of lysozyme might be described by a two-state model[12] in which the closed and open conformations are represented by the WT crystal structure (closed) and structures 172L or 173L (open). We have shown previously that in the case where multiple, rapidly inter-converting conformations exist, the relative domain orientation determined by dipolar couplings reflects a population-weighted average.[29] Assuming this two-state model, populations of open and closed states for WT* have been determined by minimizing the difference between experimental dipolar couplings and those predicted for the open and closed states using SSIA,[51] as discussed in Materials and Methods. The solution structure of WT* can be described as containing approximately equal contributions from open and closed conformers. In addition, a lower limit for the rate of interconversion between the two states can be obtained by examining ^{15}N-^1H HSQC correlation spectra of WT* and T4SS. Only a single set of peaks is observed in each spectrum, with the largest difference in shifts (0.8 ppm in ^1H) obtained for linker residue Val75. Assuming that the shifts in WT* spectra are weighted equally from contributions from open and closed states, while the shifts for T4SS correspond to those of the closed state, the rate of interdomain closure exceeds approximately 6000 s^{-1}. Evidence for interdomain dynamics on the micro- to nanosecond time-scale has been obtained from EPR studies of spin-labeled lysozyme,[11,59] although an alternative interpretation of these results in terms of variability in the conformation of the disulfide-linked nitroxide side-chain has been put forward.[60] Molecular dynamics (MD) studies of T4 lysozyme provide evidence that domain closure may be rapid, with transitions from very open to maximally closed structures occurring on the nanosecond time-scale.[26,58,61,62] Spin relaxation studies probing domain dynamics are currently in progress in our laboratory.

It is noteworthy that two-state models do not give a statistical improvement in fit between experimental and predicted dipolar couplings. It is therefore not possible to distinguish between static and dynamic models for ligand-free T4 lysozyme in solution on the basis of the dipolar coupling data and the analyses presented here. Nevertheless, it is clear that even with the limited numbers of dipolar couplings measured for WT* and T4SS, it is possible to determine average solution conformations and to establish that these conformers are significantly different from those observed by crystallography. It is anticipated that as the database of domain structure accumulates, dipolar couplings will become even more powerful in the description of domain orientation and of functionally relevant conformational changes for a wide range of multi-domain proteins.

Materials and Methods

Sample preparation

All samples of T4 lysozyme were either ^{15}N or ^{15}N, ^{13}C-labeled by expression in M9 minimal medium with ^{15}N-labeled ammonium chloride and ^{13}C-labeled glucose, and purified according to published methods.[16] Lysozyme protein concentrations were determined by absorbance readings at 280 nm, using a molar extinction coefficient of 24 170 M^{-1} cm^{-1}.[63] Experiments performed on WT* lysozyme in this study refer to the cysteine-free mutant C54T/C97A, which has wild-type activity and structure.[41] The native cysteine residues of the disulfide mutant, T21C/T142C (T4SS), were also mutated as in WT*. Spontaneous formation of the interdomain disulfide bond was confirmed by SDS-PAGE[41] and ^1H-^{15}N HSQC spectra.

Bicelle samples were made using premixed 3:1 (molar ratio) 1,2-dimyristoyl-sn-glycero-3-phosphocholine/1,2-dihexanoyl-sn-glycero-3-phosphocholine (Avanti Polar Lipids). Tetradecyl trimethylammonium bromide (TTAB) was added to a molar ratio of 30:1 total lipid to TTAB to help prevent phase separation of the bicelles.[64] A concentrated bicelle stock solution was made by adding 250 μl of lysozyme buffer (50 mM potassium phosphate (pH 5.5), 0.01 % (w/v) sodium azide, 10 % ^2H_2O) to a 50 mg vial of premixed bicelles with 2.75 μmol of TTAB (11 μl of a 250 mM TTAB stock). This mixture was incubated at 18 °C for about 30 minutes with occasional vortex mixing, followed by temperature cycling between 40 °C and 0 °C three times for one minute each.

Alignment was monitored by the quadrupole splitting of the deuterium ^2H_2O signal: 5-7.5 % (w/v) bicelle solutions formed a nematic phase at 33 °C that was stable for more than a month. The ^1HN-^{15}N dipolar couplings were measured, as described below, on samples aligned under a variety of conditions. Specifically, dipolar couplings were originally measured on a WT*-bicelle sample containing 0.5 mM ^{15}N-labeled WT* lysozyme and 7.5 % (w/v) bicelles in lysozyme buffer (high BC). The sample was then diluted to 5 % (w/v) bicelles (BC), followed by addition of sodium chloride to 150 mM (BC + salt). At each stage, dipolar couplings were obtained, resulting in three different data sets. Dipolar couplings were also measured on a 1.5 mM ^{15}N,^{13}C-labeled WT* sample aligned using a 1:1 (w/w) cetylpyridinium chloride (CPCl)/hexanol mixture in lysozyme buffer with 200 mM NaCl (3.4 % (weight of CPCl + hexanol/total volume of solution)), 25 °C.[43] Bicelle and CPCl liquid crystal samples were prepared for ^{15}N-labeled T4SS in the same way, omitting the initial 7.5 % bicelle solution. T4SS protein concentrations were 0.6 mM in the bicelle samples (BC and BC + salt) and 0.2 mM in the CPCl liquid crystal sample (CPCl). The behavior of this CPCl sample was unusual, in that it took a long period of time to achieve alignment (in excess of ten hours) and was not as phase-stable as previous preparations. The alignment tensor rhombicity in this sample was also atypically high. A summary of the samples used to measure dipolar couplings is provided in Table 1.

Data collection and analysis

All dipolar coupling spectra were recorded on a Varian Inova 600 MHz spectrometer, while assignment data were collected with Varian UnityPlus and Inova 500 MHz spectrometers. Backbone chemical shift assignments are available for WT[15,16] and T4SS (unpublished results) lysozyme and assignments for WT* were confirmed using 3D HNCACB, HBCBCACONNH and HNCO experiments (reviewed by Sattler *et al.*).[65]

Dipolar couplings for ^{15}N-labeled samples were recorded using a 2D IPAP-type ^{15}N-^{1}HN HSQC correlation experiment. The IPAP strategy records $^{1}J_{HN}$-separated doublets that are either in-phase (IP) or anti-phase (AP), which are then combined to give spectra containing only upfield or downfield components.[45,46] The pulse sequences used in these experiments are similar to previously published versions, except that gradient-enhanced sensitivity is included.[66,67] In practice, a small (5 %) multiplicative correction factor was required prior

to addition of IP and AP spectra so that only a single doublet component was present in each spectrum.[46] All 2D IPAP experiments were recorded with (296, 576) complex points and (t_1,t_2) acquisition times of (149.4 ms, 64 ms) using 16-32 transients/FID. Final data sets comprised (1024,4096) real points with a digital resolution of (1.9 Hz/pt, 2.2 Hz/pt) in (F_1,F_2). Spectra of both WT* and T4SS were recorded in duplicate at 33 °C for the aligned state in bicelles, at 25 ° C in CPCl liquid crystals and at 25 °C in the absence of any aligning medium.

^{1}HN-^{15}N dipolar couplings were also recorded on an ^{15}N, ^{13}C-labeled WT* sample (using CPCl as the alignment medium) with a 3D HNCO experiment modified to include IPAP-type separation of doublet components as described above. In this experiment (see Figure 8), the IPAP selection sequence was inserted into the regular HNCO scheme just prior to acquisition of ^{15}N chemical shift (in t_2). Data sets of (64, 38, 512) complex points and acquisition times of (45.2 ms, 31.7 ms, 64.0 ms) were collected in (t_1, t_2, t_3). IP and AP experiments were collected
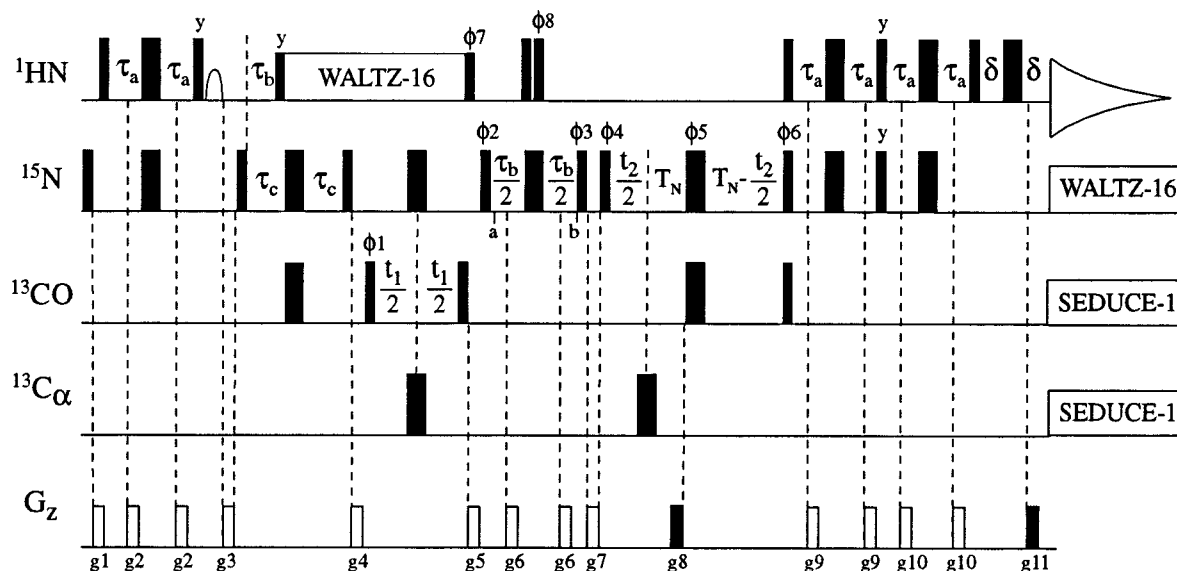

Figure 8. Pulse sequence for the measurement of ^{15}N-^{1}HN one-bond dipolar couplings in ^{15}N, ^{13}C-labeled proteins. This scheme is based on the original HNCO experiment, which has been described in detail elsewhere,[81,82] with an IPAP selection sequence[45,46] between (a) and (b) similar to that described in Yang *et al.*[83] Narrow (wide) pulses correspond to a 90° (180°) flip angle along the x axis unless indicated otherwise. The ^{1}H, ^{13}C and ^{15}N carriers are placed at 4.7 (water), 176 and 119 ppm, respectively. A 35 kHz field was used for all proton pulses except for the 1.8 ms water selective 90° flip back pulse prior to gradient g3, the WALTZ decoupling elements[84] and the flanking pulses (6.2 kHz). ^{15}N pulses were applied with a 6.2 kHz field and decoupling during acquisition was achieved with a 1 kHz field. All ^{13}C rectangular 90° (180°) pulses are applied with a field strength of $\Delta/\sqrt{15}$ ($\Delta/\sqrt{3}$), where Δ is the separation between the centers of the ^{13}C$^{\alpha}$ and ^{13}CO chemical shift regions.[85] The C$^{\alpha}$ 180° pulses are phase modulated by 118 ppm.[86,87] Prior to acquisition, the carbon carrier is jumped to 117 ppm (midway between ^{13}C$^{\alpha}$ and ^{13}CO) with SEDUCE-1[88] decoupling applied during acquisition (350 μs 90° pulses) using cosine modulation of the waveform so that both ^{13}C$^{\alpha}$ and ^{13}CO spins are affected.[89] The delays used are $\tau_a = 2.3$ ms, $\tau_b = 5.5$ ms, $\tau_c = 12.4$ ms, $T_N = 16.7$ ms, $\delta = 500$ μs. Phase cycling used to obtain the IP signal modulated according to $\cos(\omega_N t_2)\cos(\pi J t_2)$ (where J is the sum of ^{15}N-^{1}HN dipolar and scalar couplings), for example, is $\phi1 = (x, -x)$, $\phi2 = 2(x),2(-x)$, $\phi3 = y$, $\phi4 = (y, -y)$, $\phi5 = (x, -x)$, $\phi6 = x$, $\phi7 = y$, $\phi8 = x$, $acq = 2(x),2(-x)$. For the AP signal [$\sin(\omega_N t_2)\sin(\pi J t_2)$], $\phi3$ is incremented by 90°, whilst $\phi7$ and $\phi8$ are increased by 180°. The IP and AP spectra are recorded in an interleaved manner, and subsequently added and subtracted to give spectra with a single multiplet component. Quadrature detection in F_1 was achieved with States-TTPI of $\phi1$,[90] with quadrature in F_2 obtained *via* the enhanced sensitivity pulsed field gradient method,[66,67] with two spectra (($g8$, $\phi6$) and ($-g8$, $\phi6 + 180°$)) recorded for each t_2 increment. The duration and strength of the gradients are: g1 = (0.5 ms, 8 G/cm), g2 = (0.5 ms, 5 G/cm), g3 = (1 ms, 15 G/cm), g4 = (0.75 ms, 20 G/cm), g5 = (0.6 ms, 12 G/cm), g6 = (0.3 ms, 10 G/cm), g7 = (0.8 ms, 20 G/cm), g8 = (1.25 ms, 30 G/cm), g9 = (0.3 ms, 4 G/cm), g10 = (0.4 ms, 7 G/cm), g11 = (0.125 ms, 29.6 G/cm). Decoupling is interrupted prior to the application of gradients.[91]

in an interleaved manner with a net acquisition time of 23 hours. The ^{15}N time domain was doubled with mirror image linear prediction,[68] giving a final data set of (128, 512, 1024) real points with a corresponding digital resolution of (11.1 Hz/pt, 2.3 Hz/pt, 7.8 Hz/pt) in (F_1, F_2, F_3). Separation of the ^{15}N-^{1}HN correlation peaks into a third dimension increased the number of dipolar couplings that could be obtained for T4 lysozyme by approximately twofold (see Table 1, last entry under WT*).

NMRPipe software[69] was used in the processing of all data sets, whilst NMRView version 3 was used in the assignment of WT* backbone chemical shifts.[70] The PIPP/CAPP suite of programs[71] was used to measure splittings in all dipolar coupling spectra. Pairwise rmsd of the dipolar couplings between duplicate data sets was 0.2-0.4 Hz for the 2D HSQC-IPAP experiments over the range of ^{15}N-labeled samples and 0.6 Hz in the 3D HNCO-IPAP data set for a 1.5 mM ^{15}N,^{13}C-labeled WT* sample where alignment was obtained in 3.4 % CPCl/hexanol liquid crystals.

Definition of rotation axes

In the domain orientation analyses, a family of nine T4 lysozyme X-ray structures were used where the resolution was 2.0 Å or better. The PDB identifiers and descriptions of these nine structures are shown in Table 2. (Note that 150L(c) and the X-ray structure of T4SS were not used in the analysis).

All vectors and rotations are described with respect to the molecular frame of the 3LZM (WT) PDB co-ordinate file.[72] All X-ray structures used in the analyses were placed in this frame by superimposing the C-domain of each structure onto the 3LZM C-domain using MOLMOL.[73] In Table 2, the relative domain orientations of these structures are described in terms of rotations required to superimpose the 3LZM N-domain onto the N-domain from the indicated structure. In all analyses, we have chosen to describe this transformation in terms of three consecutive rotations about a set of orthogonal axes, closure, bend and twist axes, given by the polar angles {63°, 161°}, {115°, 85°} and {142°, 31°}, respectively. Note that this order differs from that used in a previous analysis of domain orientation in the maltose binding protein (MBP) that performed the rotations in the order of closure, twist and bend.[29] The twist axis used for lysozyme connects the centers of mass of the two domains in the WT (3LZM) structure. The closure axis was defined, using the hinge axis about which a single rotation is performed to convert the closed 3LZM structure into the open 172L structure. This vector was orthogonalized with respect to the twist axis to give the axis of closure. The cross-product of unit vectors along the twist and closure axes (twist vector × closure vector) defines a unit vector parallel with the bend axis. The use of a single rotation axis system to describe all conformational changes with respect to a known reference structure allows a simple and direct comparison of rotation parameters between structures. In addition, in the absence of electrostatic interactions between the protein and aligning media (i.e. purely steric alignment), the long axis of the alignment tensor will be expected to roughly coincide with the twist axis, which sequesters a large part of the experimental uncertainty into this dimension (see the text).

Calculation of domain orientations

Determination of relative domain orientations using dipolar couplings was performed with a modified version of Conformist1.0.[29] Prior to the analysis, all input X-ray structures (Table 2) were split into isolated N and C-domains that were superimposed on the N and C-domain respectively, of the reference X-ray structure. For analyses using dipolar couplings measured on WT*, the closed WT structure 3LZM was chosen as the reference structure, while the X-ray coordinates of T4SS rotated into the 3LZM molecular frame (i.e. with the C-domains of T4SS and WT superimposed) were used as the reference structure in calculations involving dipolar couplings from T4SS.

In the procedure employed here, the experimental backbone ^{15}N-^{1}HN dipolar couplings for each domain are fit to those calculated on a domain basis from the X-ray co-ordinates using equation (2):

$$D_{NH} = -\frac{\gamma_H \gamma_N \hbar}{2\pi r_{NH}^3} A_a \left[(3\cos^2\theta - 1) + \frac{3}{2} R \sin^2\theta \cos 2\phi \right] \quad (2)$$

where the polar angles {θ, φ} give the orientation of the ^{15}N-^{1}HN internuclear vector with respect to the alignment frame and A_a and R are the axial and rhombic components of the alignment tensor, respectively. The Euler angles {α, β, γ} give the orientation of the alignment tensor with respect to the molecular frame which for all analyses is the PDB frame for the crystal structure 3LZM. For each domain, singular value decomposition is used to calculate the alignment tensor parameters A_a, R, α, β, γ.[29,56] The Euler angles obtained from the N and C-domain analyses are used to calculate the rotation matrix that transforms the 3LZM N-domain orientation into the relative domain orientation determined from the dipolar couplings measured in solution. Hinge rotation parameters {Θ, Φ, Ω}, are then determined from the elements in this matrix, where {Θ, Φ} are the polar angles that give the orientation of the hinge axis in the co-ordinate frame of the reference structure and Ω is the amplitude of rotation about that axis.[29,74] These parameters are then recast in terms of consecutive rotations about the closure, bend and twist axes described above. The rotations, in turn, give the relative domain orientation in solution as obtained from the dipolar couplings with respect to the reference X-ray structure. In the event that the average relative domain orientation of the molecule in solution is represented accurately by the relative domain orientation in the reference structure, then the closure, bend and twist angles are {0°, 0°, 0°}.

For each member of the family of input structures (Table 2), the relative domain orientation computation was performed 100 times, with 10 % of the experimental dipolar couplings removed at random each time. This jack-knife procedure[75] permitted the estimation of variability in closure, bend and twist that results from errors in the dipolar coupling values. Average closure, bend and twist angles were calculated over all 100 trials for each structure to give the final results represented in Figures 2 and 4 by the filled circles. The error bars associated with each point represent the corresponding standard deviation over the 100 trials. The average values for the closure, bend and twist angles that were obtained from each of the nine input crystal structures were then used to calculate the mean relative domain orientation for a particular aligning medium as reported in Table 3. The impact of intradomain structural noise on this result is given by the standard deviation calculated

over the nine structures and reported as the error in Table 3. This domain orientation procedure was performed for each set of dipolar couplings obtained under the different alignment conditions listed in Table 1.

Evaluation of domain dynamics

The domain orientation procedure described above is based on the assumption that the dynamic properties of the two domains are equivalent.[29,37] Hence the alignment tensor parameters A_a and R determined for each of the domains independently should be the same. To evaluate whether this is the case for T4 lysozyme, average values of A_a for the N and C-domains (A_a^C and A_a^N, respectively) were calculated using the domain orientation procedure described above. For each of the nine X-ray structures and each set of dipolar couplings, the percentage difference in A_a between domains was calculated according to the relation:

$$100 \times \frac{(A_a^C - A_a^N)}{A_a^{mean}}, A_a^{mean} = \frac{(A_a^C + A_a^N)}{2} \qquad (3)$$

We found that, depending on the structure and the set of dipolar couplings used, the A_a values determined for each of the two domains could vary somewhat. Average differences in A_a values between N and C-domains computed from the dipolar couplings measured for WT* over all nine input X-ray structures ranged from $4\% \pm 6\%$ (BC + salt), to $7\% \pm 5\%$ (CPCl) and for T4SS from $-4\% \pm 7\%$ (BC) to $10\% \pm 6\%$ (CPCl).

To evaluate the possibility that the observed differences in A_a could arise from small variations in intradomain structure between crystal and solution states of lysozyme a similar analysis was performed using simulated dipolar couplings in place of the experimental data sets. Specifically, a set of dipolar couplings was calculated using the X-ray structures 150L(a) and 150L(c) with the alignment tensor parameters $A_a = 0.0015$, $R = 0.1709$ and $\{\alpha, \beta, \gamma\} = \{186°, 142°, 53°\}$. Using simulated dipolar couplings only from those residues for which couplings had been measured on WT* lysozyme in the BC aligning medium (38 and 28 couplings from the C and N-domain, respectively) the domain orientation procedure described above was performed. When the set of couplings constructed from structure 150L(a) was used, the average difference in A_a values over the set of nine input X-ray structures is $11\% \pm 8\%$. However, if the structure 150L(c) was used to simulate dipolar couplings instead, a difference of $-7\% \pm 8\%$ is obtained. Although the differences in intradomain structure between the different X-ray structures listed in Table 2 are small (backbone pairwise rmsd of ca 0.1-0.6 Å), the range in A_a calculated for each of the two domains are similar to what is observed when experimental data are used. Additionally, the backbone pairwise rmsd between intradomain X-ray structures 150L(a) and 150L(c) is 0.6 Å and yet sizeable differences in A_a values are obtained when alignment parameters are calculated from each set of simulated dipolar couplings. This suggests that the differences in alignment parameters obtained on the basis of the experimental data may not reflect differential dynamics between domains, but rather subtle changes in intradomain structure in concert with only a limited number of dipolar coupling measurements. Notably, when the number of dipolar couplings used in the simulations increases to include values from all residues the difference in A_a values between domains decreases to $3\% \pm 4\%$ and $4\% \pm 4\%$ for couplings simulated from

150L(a) and 150L(c), respectively. Evidence that the two domains of lysozyme are dynamically similar is provided by steady-state ^{15}N-^{1}H NOE values, which are essentially the same between the two domains (average values of 0.74 ± 0.03 and 0.76 ± 0.04 for N and C-domains, respectively).

Resolving degeneracies in solutions

As noted in previous studies of two-domain proteins, there is a 4-fold degeneracy in relative domain orientation calculated from dipolar couplings measured in a single aligning medium.[29,37] However, if the reference structure is related to the liquid-state conformation by a small amplitude rotation, then it is straightforward to identify the correct solution, since all other rotations are of large (and very likely unphysical) amplitude (Ω of the order of 180°).[29] Large differences between lysozyme solution and crystal conformations were not anticipated, and consequently the orientation corresponding to the smallest amplitude rotation (i.e. lowest Ω) was used in all analyses. However, it should be noted that when the magnitude of Ω exceeds about 70°, the amplitude of hinge rotations given by degenerate solutions can become comparable in size. This was observed when dipolar couplings measured on T4SS aligned using bicelles were analyzed with the structures 172L and 152L. In all cases, removal of structural elements that agree poorly with the measured dipolar couplings (the N-terminal α-helix in these two cases) re-established solutions with small-amplitude rotations.

That the small amplitude Ω results correspond to the actual solution conformation is supported by the fact that similar orientations are obtained from different aligning media (Table 3). We performed an analysis similar to the procedure of Hashimi *et al.*[76] to rule out the possibility that one of the other three solutions represents the actual solution conformation of lysozyme. First, the solution conformations were constructed for the four degenerate solutions from each aligning medium (procedure described in the next section). Then the C-domains were all overlaid and armsd (pairwise angle root-mean-squared deviation) values calculated for backbone ^{1}HN-^{15}N internuclear bond vectors of the N-domains obtained from the different aligning media. Using this procedure, the best agreement is obtained between structures arising from small Ω (1.4° armsd) *versus* large Ω (2.6°-4.7° armsd) values even when there is only a 4° difference in the orientation of the long axis of the alignment tensor (high BC and BC for WT*). Larger differences between alignment tensor long axes (e.g. 14° between BC + salt and CPCl) lead to increased armsd values between the different solutions (4.8° for small Ω, 8.9°-18° for other solutions).

Building a solution conformation

It is possible to reconstruct a solution conformation of T4 lysozyme using the reference crystal structure and the output of the domain orientation procedure described above (Table 3). In this process, one domain of the crystal structure is held fixed while a rigid-body transformation is applied to the other domain. The transformation of the coordinates of the N-domain, $\{\vec{v}_i\}$, from the reference crystal structure to the solution structure, $\{\vec{v}_i'\}$, is given by:

$$\vec{v}' = \tilde{R} \times (\vec{v} - \vec{p}) + \vec{p} + T\vec{n} \qquad (4)$$

where the rotation matrix $\tilde{R}$ and the hinge axis of rotation $\vec{n}$ are orientational parameters that are obtained directly from the domain orientation procedure. This expression also contains terms that describe the position of the vector, $\vec{v}'$ (as opposed to the orientation), in the form of $\vec{p}$ (pivot), which gives the location of the hinge axis, and T, which is the magnitude of the translation along the hinge axis $\vec{n}$.[57,74]

The parameters defining the position of the transformed vector are not provided by dipolar coupling data but can be estimated from a pair of representative open and closed lysozyme crystal structures using equation (4). For example, if the C-domains from the open and closed crystal structures are superimposed and the closed form taken as the starting conformation, then the open structure can be considered to represent the result of a rigid-body transformation of the N-domain of the closed structure as given by equation (4). Consequently, both $\vec{v}$ and $\vec{v}'$ are defined for all atoms in the N-domain. In our analysis, after the C-domains of the open and closed X-ray structures were overlaid, the rotation parameters required to superimpose the N-domain of the closed structure onto that of the open structure were obtained using MOLMOL.[73] The translation (T) was subsequently calculated from the relation:

$$T = (\vec{v}' - \vec{v}) \cdot \vec{n} \qquad (5)$$

and the pivot location determined by solving equation (4) for $\vec{p}$. In practice, we have used vectors extending from the origin to the centers of mass of the N-domains of the closed and open X-ray structures in the calculation of T and $\vec{p}$ to minimize contributions to the transformation from differences in intradomain structure between the two forms. Using 3LZM and 150L(c) as the closed and open structures, respectively, a pivot location of {1.7, −4.3, 5.0} and a 2.2 Å translation (moving away from the C-domain) were obtained. Similar positional parameters result from other pairs of open and closed lysozyme structures so long as the hinge axes, $\vec{n}$, are close to coincident. In line with previous observations,[12] we found that this was generally the case when there was more than 10° closure relating the two forms.

The orientation of the hinge axis that transforms the N-domain of 3LZM into the solution conformation of WT* lysozyme as determined from the dipolar couplings was found to be similar to the crystallographic hinge described above (e.g. 4°-10° between the solution and X-ray hinges for bicelle media and 26° for results from CPCl media). Therefore, the pivot and translation obtained from the above analysis have been used in the reconstruction of the WT* solution conformation.

Solution conformations were generated from the X-ray coordinates for the N-domain of the reference structure (3LZM) by applying the rotation (established from the dipolar couplings, see Table 3) and the translation parameters as described above using equation (4). As shown in Figure 3, the reconstructed solution conformation consists of the original C-domain and the transformed N-domain. The structure of the intervening linker region is not obtained by this approach and is therefore not represented.

The T4SS solution conformations in Figure 5 were reconstructed as indicated above, except that the X-ray coordinates for T4SS instead of 3LZM were used. As described in Discussion, the solution structure of T4SS is significantly more closed then even the most closed X-ray structure in the data base, 152L, and it is consequently difficult to obtain suitable values for T and $\vec{p}$

in this case. We have therefore used the pivot position obtained from analysis of the dipolar couplings from WT* and set $T = 0$. However, in some cases the hinge axis predicted from dipolar coupling data is significantly different from the crystallographic hinge described above and the positional degrees of freedom used for the T4SS structures are likely to be incorrect. With this in mind, an alternative procedure for obtaining solution structures of T4SS was employed (see the next section).

Rigid-body minimization

Models of the solution conformation of T4SS were also generated using an algorithm implemented within the structure calculation program CNS[52] that uses dipolar couplings to reorient domains of a lysozyme crystal structure. In order to minimize structural distortion of the domains during the refinement procedure, an extensive set of intradomain restraints was generated based on the backbone coordinates of the starting structure. Starting coordinates were obtained from a lysozyme crystal structure using standard protonation and refinement protocols.[52] Distance restraint lists involving all HN-HN and N-N pairs within each domain of lysozyme were constructed. In addition, N-O distances were restrained according to the hydrogen bonding network within the domains as determined by the program hbplus.[77] Backbone dihedral angles were also used as input for the refinement procedure.

Experimental residual dipolar couplings were included in structure calculations using the CNS module described by Clore *et al.*[78] Alignment parameters (D_a and R of 12.85 and 0.15, respectively) were estimated from direct fitting of the experimental couplings to several sets of crystallographic coordinates. An artificial tetra-atomic molecule representing the set of alignment axes[78] was placed 200 Å away from the origin and oriented according to the alignment axes of the C-domain of the starting protein structure. The orientation of this pseudo-molecule was allowed to float during the torsional angle dynamics period of the refinement protocol. The set of dipolar couplings measured on T4SS in bicelles, which includes several couplings from the linker region, were used as input. The force constant for dipolar couplings was ramped from 0.05 to 0.5 kcal/mol Hz² (for HN-type couplings; 1 kcal = 4.184 kJ).[79]

In the procedure implemented in our study, a low-temperature torsional angle dynamics simulated annealing stage was first performed[79,80] followed by a standard conjugate gradient minimization. In this approach the system is cooled from 200 K to 0 K in steps of 5 K and 15 ps of molecular dynamics at each temperature step are performed with a time-step of 3 fs. Distance and hydrogen-bonding restraints are enforced by a parabolic potential with a force constant of 200 kcal/mol Å² and a narrow flat region (±0.01 Å). Likewise, backbone dihedral angles within the domains are restrained using a steep parabolic potential (5000 kcal/mol rad²; ±0.1°). Using these force constants, contributions to the penalty function from distance and dihedral angle terms are approximately equal. In addition, the van der Waals force constant is ramped from 0.1 to 1 kcal/mol Å². Following the low-temperature simulated annealing stage, the structure is refined using ten cycles of conjugate gradient minimization with the force constants of 150 kcal/mol Å² and 600 kcal/mol rad² for distance and dihedral angle restraints, respectively.

In line with expectations, the internal structure of the domains is not significantly perturbed during the course of the refinement procedure (backbone intradomain rmsd values between starting and final structures were less than 0.05 Å). At the same time, closure and bend (relative to the reference X-ray conformation of T4SS) are within 3° of values obtained using the Conformist1.0 software (the ill-defined twist component may differ by as much as 6°). Multiple structures derived from the same set of the starting coordinates are very similar, with less than 1° difference in closure, bend and twist values between the different structures in the ensemble.

Calculations using a two-state model

The experimental dipolar couplings can also be fit to a two-state model in which an open and a closed structure are assumed to be rapidly interconverting.[29] A set of dipolar couplings was simulated for representative open (D_{open}^{calc}) and closed (D_{closed}^{calc}) structures, with alignment parameters of each state predicted from the steric model of alignment using SSIA.[52] The fraction of lysozyme that is in the closed state (p_{closed}) is obtained by minimizing the difference between calculated dipolar couplings arising from this two-state process, $D_{2\text{-state}}^{calc}$:

$$D_{2\text{-state}}^{calc} = p_{closed} \times D_{closed}^{calc} + (1 - p_{closed}) \times D_{open}^{calc} \quad (6)$$

and the experimental set of dipolar couplings.

The population of the closed form in this two-state model was calculated using the measured set of dipolar couplings obtained from WT* lysozyme in the BC + salt aligning medium using the X-ray structure 3LZM as a model for the closed conformation, whilst the open conformation was represented by X-ray structure 172L or 173L. To reduce the potential effect of differences in intradomain structure between the different crystal forms of lysozyme on the extracted populations, each of the two domains of the 3LZM structure was superimposed onto the corresponding domains of the structures representing the open form and the resulting structure used in the calculation of D_{open}^{calc}. However, the alignment tensor parameters predicted from SSIA that were used to calculate D_{open}^{calc} were obtained using the original crystal structure of the representative open form.

Acknowledgments

References

1. Tsugita, A. (1971). *The Enzymes* (Boyer, P. D., ed.), 3rd edit., vol. 5, Academic Press, New York.

2. Jensen, H. B., Kleppe, G., Schindler, M. & Mirelman, D. (1976). The specificity requirements of bacteriophage T4 lysozyme. *Eur. J. Biochem.* **66**, 319-325.

3. Mirelman, D., Kleppe, G. & Jensen, H. B. (1975). Studies on the specificity of action of bacteriophage T4 lysozyme. *Eur. J. Biochem.* **55**, 369-363.

4. Kuroki, R., Weaver, L. H. & Matthews, B. W. (1993). A covalent enzyme-substrate intermediate with saccharide distortion in a mutant T4 lysozyme. *Science,* **262**, 2030-2033.

5. Hardy, L. W. & Poteete, A. R. (1991). Reexamination of the role of Asp20 in catalysis by bacteriophage T4 lysozyme. *Biochemistry,* **30**, 9457-9463.

6. Anderson, W. F., Grutter, M. G., Remington, S. J., Weaver, L. H. & Matthews, B. W. (1981). Crystallographic determination of the mode of binding of oligosaccharides to T4 bacteriophage lysozyme: implications for the mechanism of catalysis. *J. Mol. Biol.* **147**, 523-543.

7. Kuroki, R., Weaver, L. H. & Matthews, B. W. (1999). Structural basis of the conversion of T4 lysozyme into a transglycosidase by reengineering the active site. *Proc. Natl Acad. Sci. USA*, **96**, 8949-8954.

8. Weaver, L. H. & Matthews, B. W. (1987). Structure of bacteriophage T4 lysozyme refined at 1.7 Å resolution. *Protein Eng.* **1**, 115-123.

9. Matthews, B. W. & Remington, S. J. (1974). The three dimensional structure of the lysozyme from bacteriophage T4. *Proc. Natl Acad. Sci. USA,* **71**, 4178-4182.

10. Timchenko, A. A., Ptitsyn, O. B., Troitsky, A. V. & Denesyuk, A. I. (1978). The structure of phage T4 lysozyme in solution noticeably differs from its crystalline struction. *FEBS Letters,* **88**, 109-113.

11. McHaourab, H. S., Lietzow, M. A., Hideg, K. & Hubbell, W. L. (1996). Motion of spin-labeled sidechains in T4 lysozyme, correlation with protein structure and dynamics. *Biochemistry,* **35**, 7692-7704.

12. Zhang, X. J., Wozniak, J. A. & Matthews, B. W. (1995). Protein flexibility and adaptability seen in 25 crystal forms of T4 lysozyme. *J. Mol. Biol.* **250**, 527-552.

13. Faber, H. R. & Matthews, B. W. (1990). A mutant T4 lysozyme displays five different crystal conformations. *Nature,* **348**, 263-266.

14. Dixon, M. M., Nicholson, H., Shewchuk, L., Baase, W. A. & Matthews, B. W. (1992). Structure of a hinge-bending bacteriophage T4 lysozyme mutant, Ile3 → Pro. *J. Mol. Biol.* **227**, 917-933.

15. Fischer, M. W., Majumdar, A., Dahlquist, F. W. & Zuiderweg, E. R. (1995). ^{15}N, ^{13}C, and ^{1}H NMR assignments and secondary structure for T4-lysozyme. *J. Magn. Reson. ser. B,* **108**, 143-154.

16. McIntosh, L. P., Wand, A. J., Lowry, D. F., Redfield, A. G. & Dahlquist, F. W. (1990). Assignment of the backbone ^{1}H and ^{15}N NMR resonances of bacteriophage T4 lysozyme. *Biochemistry,* **29**, 6341-6362.

17. Yang, G. L., Cecconi, C., Baase, W. A., Vetter, I. R., Breyer, W. A., Haack, J. A., Matthews, B. W., Dahlquist, F. W. & Bustamante, C. (2000). Solid-state synthesis and mechanical unfolding of polymers of T4 lysozyme. *Proc. Natl Acad. Sci. USA,* **97**, 139-144.

18. Llinas, M. & Marqusee, S. (1998). Subdomain interactions as a determinant in the folding and stability of T4 lysozyme. *Protein Sci.* **7**, 96-104.

19. Kuroki, R., Weaver, L. H. & Matthews, B. W. (1995). Structure-based design of a lysozyme with altered catalytic activity. *Nature Struct. Biol.* **2**, 1007-1011.

20. Eriksson, A. E., Baase, W. A., Wozniak, J. A. & Matthews, B. W. (1992). A cavity-containing mutant of T4 lysozyme is stabilized by buried benzene. *Nature,* **355**, 371-373.

21. Mulder, F. A., Hon, B., Muhandiram, D. R., Dahlquist, F. W. & Kay, L. E. (2000). Flexibility and ligand exchange in a buried cavity mutant of T4 lysozyme studied by multinuclear NMR. *Biochemistry,* **39**, 12614-12622.

22. Gassner, N. C. & Matthews, B. W. (1999). Use of differentially substituted selenomethionine proteins in X-ray structure determination. *Acta Crystallog. sect. D,* **55**, 1967-1970.

23. Bell, J. A., Wilson, K. P., Zhang, X. J., Faber, H. R., Nicholson, H. & Matthews, B. W. (1991). Comparison of the crystal structure of bacteriophage T4 lysozyme at low, medium, and high ionic strengths. *Proteins: Struct. Funct. Genet.* **10**, 10-21.

24. McIntosh, L. P., Griffey, R. H., Muchmore, D. C., Nielson, C. P., Redfield, A. G. & Dahlquist, F. W. (1987). Proton NMR measurements of bacteriophage T4 lysozyme aided by ^{15}N isotopic labeling: structural and dynamic studies of larger proteins. *Proc. Natl Acad. Sci. USA,* **84**, 1244-1248.

25. Hall, D. A., Maus, D. C., Gerfen, G. J., Inati, S. J., Becerra, L. R., Dahlquist, F. W. & Griffin, R. G. (1997). Polarization-enhanced NMR spectroscopy of biomolecules in frozen solution. *Science,* **276**, 930-932.

26. Bahar, I., Erman, B., Haliloglu, T. & Jernigan, R. L. (1997). Efficient characterization of collective motions and interresidue correlations in proteins by low-resolution simulations. *Biochemistry,* **36**, 13512-13523.

27. vanAalten, D. M. F., Conn, D. A., deGroot, B. L., Berendsen, H. J. C., Findlay, J. B. C. & Amadei, A. (1997). Protein dynamics derived from clusters of crystal structures. *Biophys. J.* **73**, 2891-2896.

28. McHaourab, H. S., Kalai, T., Hideg, K. & Hubbell, W. L. (1999). Motion of spin-labeled side-chains in T4 lysozyme: effect of side-chain structure. *Biochemistry,* **38**, 2947-2955.

29. Skrynnikov, N. R., Goto, N. K., Yang, D., Choy, W. Y., Tolman, J. R., Mueller, G. A. & Kay, L. E. (2000). Orienting domains in proteins using dipolar couplings measured by liquid-state NMR: differences in solution and crystal forms of maltodextrin binding protein loaded with beta-cyclodextrin. *J. Mol. Biol.* **295**, 1265-1273.

30. Tjandra, N., Omichinski, J. G., Gronenborn, A. M., Clore, G. M. & Bax, A. (1997). Use of dipolar [1]H-^{15}N and [1]H-^{13}C couplings in the structure determination of magnetically oriented macromolecules in solution. *Nature Struct. Biol.* **4**, 732-738.

31. Tjandra, N. & Bax, A. (1997). Measurement of dipolar contributions to $^1J_{CH}$ splittings from magnetic-field dependence of J modulation in two-dimensional NMR spectra. *J. Magn. Reson.* **124**, 512-515.

32. Al-Hashimi, H. M., Bolon, P. J. & Prestegard, J. H. (2000). Molecular symmetry as an aid to geometry determination in ligand protein complexes. *J. Magn. Reson.* **142**, 153-158.

33. Prestegard, J. H. (1998). New techniques in structural NMR - anisotropic interactions. *Nature Struct. Biol.* **5**, 517-522.

34. Bayer, P., Varani, L. & Varani, G. (1999). Refinement of the structure of protein-RNA complexes by residual dipolar coupling analysis. *J. Biomol. NMR,* **14**, 149-155.

35. Tjandra, N., Tate, S., Ono, A., Kainosho, M. & Bax, A. (2000). The NMR structure of a DNA dodecamer in an aqueous dilute liquid crystalline phase. *J. Am. Chem. Soc.* **122**, 6190-6200.

36. Mueller, G. A., Choy, W. Y., Yang, D. W., Forman-Kay, J. D., Venters, R. A. & Kay, L. E. (2000). Global folds of proteins with low densities of NOEs using residual dipolar couplings: application to the 370-residue maltodextrin-binding protein. *J. Mol. Biol.* **300**, 197-212.

37. Fischer, M. W., Losonczi, J. A., Weaver, J. L. & Prestegard, J. H. (1999). Domain orientation and dynamics in multidomain proteins from residual dipolar couplings. *Biochemistry,* **38**, 9013-9022.

38. Clore, G. M. (2000). Accurate and rapid docking of protein-protein complexes on the basis of intermolecular nuclear overhauser enhancement data and dipolar couplings by rigid body minimization. *Proc. Natl Acad. Sci. USA,* **97**, 9021-9025.

39. Markus, M. A., Gerstner, R. B., Draper, D. E. & Torchia, D. A. (1999). Refining the overall structure and subdomain orientation of ribosomal protein S4 Δ41 with dipolar couplings measured by NMR in uniaxial liquid crystalline phases. *J. Mol. Biol.* **292**, 375-387.

40. Biekofsky, R. R., Muskett, F. W., Schmidt, J. M., Martin, S. R., Browne, J. P., Bayley, P. M. & Feeney, J. (1999). NMR approaches for monitoring domain orientations in calcium-binding proteins in solution using partial replacement of Ca^{2+} by Tb^{3+}. *FEBS Letters,* **460**, 519-526.

41. Matsumura, M. & Matthews, B. W. (1989). Control of enzyme activity by an engineered disulfide bond. *Science,* **243**, 792-794.

42. Tjandra, N. & Bax, A. (1997). Direct measurement of distances and angles in biomolecules by NMR in a dilute liquid crystalline medium. *Science,* **278**, 1111-1114.

43. Prosser, R. S., Losonczi, J. A. & Shiyanovskaya, I. V. (1998). Use of a novel aqueous liquid crystalline medium for high-resolution NMR of macromolecules in solution. *J. Am. Chem. Soc.* **120**, 11010-11011.

44. Barrientos, L. G., Dolan, C. & Gronenborn, A. M. (2000). Characterization of surfactant liquid crystal phases suitable for molecular alignment and measurement of dipolar couplings. *J. Biomol. NMR,* **16**, 329-337.

45. Yang, D. W. & Nagayama, K. (1996). A sensitivity-enhanced method for measuring heteronuclear long-range coupling constants from the displacement of signals in two 1D subspectra. *J. Magn. Reson. ser. A,* **118**, 117-121.

46. Ottiger, M., Delaglio, F. & Bax, A. (1998). Measurement of J and dipolar couplings from simplified two-dimensional NMR spectra. *J. Magn. Reson.* **131**, 373-378.

47. Hubbell, W. L., Cafiso, D. S. & Altenbach, C. (2000). Identifying conformational changes with site-directed spin labeling. *Nature Struct. Biol.* **7**, 735-739.

48. McHaourab, H. S., Oh, K. J., Fang, C. J. & Hubbell, W. L. (1997). Conformation of T4 lysozyme in solution. Hinge-bending motion and the substrate-induced conformational transition studied by site-directed spin labeling. *Biochemistry,* **36**, 307-316.

49. Jacobson, R. H., Matsumura, M., Faber, H. R. & Matthews, B. W. (1992). Structure of a stabilizing

disulfide bridge mutant that closes the active-site cleft of T4 lysozyme. *Protein Sci.* **1**, 46-57.

50. Thornton, J. M. (1981). Disulfide bridges in globular proteins. *J. Mol. Biol.* **151**, 261-287.

51. Zweckstetter, M. & Bax, A. (2000). Prediction of sterically induced alignment in a dilute liquid crystalline phase: aid to protein structure determination by NMR. *J. Am. Chem. Soc.* **122**, 3791-3792.

52. Brunger, A. T., Adams, P. D., Clore, G. M., DeLano, W. L., Gros, P., Grosse-Kunstleve, R. W., Jiang, J. S., Kuszewski, J., Nilges, M., Pannu, N. S., Read, R. J., Rice, L. M., Simonson, T. & Warren, G. L. (1998). Crystallography & NMR system: a new software suite for macromolecular structure determination. *Acta Crystallog. sect. D*, **54**, 905-921.

53. Ojennus, D. D., Mitton-Fry, R. M. & Wuttke, D. S. (1999). Induced alignment and measurement of dipolar couplings of an SH2 domain through direct binding with filamentous phage. *J. Biomol. NMR,* **14**, 175-179.

54. Sass, J., Cordier, F., Hoffmann, A., Cousin, A., Omichinski, J. G., Lowen, H. & Grzesiek, S. (1999). Purple membrane induced alignment of biological macromolecules in the magnetic field. *J. Am. Chem. Soc.* **121**, 2047-2055.

55. Koenig, B. W., Hu, J. S., Ottiger, M., Bose, S., Hendler, R. W. & Bax, A. (1999). NMR measurement of dipolar couplings in proteins aligned by transient binding to purple membrane fragments. *J. Am. Chem. Soc.* **121**, 1385-1386.

56. Losonczi, J. A., Andrec, M., Fischer, M. W. & Prestegard, J. H. (1999). Order matrix analysis of residual dipolar couplings using singular value decomposition. *J. Magn. Reson.* **138**, 334-342.

57. Hayward, S. & Berendsen, H. J. C. (1998). Systematic analysis of domain motions in proteins from conformational change: new results on citrate synthase and T4 lysozyme. *Proteins: Struct. Funct. Genet.* **30**, 144-154.

58. de Groot, B. L., Hayward, S., van Aalten, D. M. F., Amadei, A. & Berendsen, H. J. C. (1998). Domain motions in bacteriophage T4 lysozyme: a comparison between molecular dynamics and crystallographic data. *Proteins: Struct. Funct. Genet.* **31**, 116-127.

59. Hustedt, E. J. & Beth, A. H. (1999). Nitroxide spin-spin interactions: applications to protein structure and dynamics. *Annu. Rev. Biophys. Biomol. Struct.* **28**, 129-153.

60. Langen, R., Oh, K. J., Cascio, D. & Hubbell, W. L. (2000). Crystal structures of spin labeled T4 lysozyme mutants: implications for the interpretation of EPR spectra in terms of structure. *Biochemistry,* **39**, 8396-8405.

61. Tuckerman, M. E. & Martyna, G. J. (2000). Understanding modern molecular dynamics: Techniques and applications. *J. Phys. Chem. ser. B,* **104**, 159-178.

62. Mann, G. & Hermans, J. (2000). Modeling protein-small molecule interactions: Structure and thermodynamics of noble gases binding in a cavity in mutant phage T4 lysozyme L99A. *J. Mol. Biol.* **302**, 979-989.

63. Tsugita, A. & Inouye, M. (1968). Purification of bacteriophage T4 lysozyme. *J. Biol. Chem.* **243**, 391-397.

64. Losonczi, J. A. & Prestegard, J. H. (1998). Improved dilute bicelle solutions for high-resolution NMR of biological macromolecules. *J. Biomol. NMR,* **12**, 447-451.

65. Sattler, M., Schleucher, J. & Griesinger, C. (1999). Heteronuclear multidimensional NMR experiments for the structure determination of proteins in solution employing pulsed field gradients. *Prog. Nucl. Magn. Reson. Spectrosc.* **34**, 93-158.

66. Kay, L. E., Keifer, P. & Saarinen, T. (1992). Pure absorption gradient enhanced heteronuclear single quantum correlation spectroscopy with improved sensitivity. *J. Am. Chem. Soc.* **114**, 10663-10665.

67. Schleucher, J., Sattler, M. & Griesinger, C. (1993). Coherence selection by gradients without signal attenuation: application to the 3-dimensional HNCO experiment. *Angew. Chem.-Int. Edit. Engl.* **32**, 1489-1491.

68. Zhu, G. & Bax, A. (1990). Improved linear prediction for truncated signals of known phase. *J. Magn. Reson.* **90**, 405-410.

69. Delaglio, F., Grzesiek, S., Vuister, G. W., Zhu, G., Pfeifer, J. & Bax, A. (1995). NMRPipe: a multidimensional spectral processing system based on UNIX pipes. *J. Biomol. NMR,* **6**, 277-293.

70. Johnson, B. A. & Blevins, R. A. (1994). Nmr view: a computer program for the visualization and analysis of NMR data. *J. Biomol. NMR,* **4**, 603-614.

71. Garrett, D. S., Powers, R., Gronenborn, A. M. & Clore, G. M. (1991). A common sense approach to peak picking in two-, three-, and four-dimensional spectra using automatic computer analysis of contour diagrams. *J. Magn. Reson.* **95**, 214-220.

72. Matsumura, M., Wozniak, J. A., Sun, D. P. & Matthews, B. W. (1989). Structural studies of mutants of T4 lysozyme that alter hydrophobic stabilization. *J. Biol. Chem.* **264**, 16059-16066.

73. Koradi, R., Billeter, M. & Wuthrich, K. (1996). MOLMOL: a program for display and analysis of macromolecular structures. *J. Mol. Graph.* **14**, 51-55.

74. Goldstein, H. (1980). *Classical Mechanics*, 2nd edit., Addison-Wesley Publishing Co., Reading, MA, USA.

75. Mosteller, F. & Tukey, J. (1977). *Data Analysis and Regression: A Second Course in Statistics*, Addison-Wesley Publishing Co., Don Mills, Ontario.

76. Al-Hashimi, H. M., Valafar, H., Terrell, M., Zartler, E. R., Eidsness, M. K. & Prestegard, J. H. (2000). Variation of molecular alignment as a means of resolving orientational ambiguities in protein structures from dipolar couplings. *J. Magn. Reson.* **143**, 402-406.

77. McDonald, I. K. & Thornton, J. M. (1994). Satisfying hydrogen bonding potential in proteins. *J. Mol. Biol.* **238**, 777-793.

78. Clore, G. M., Gronenborn, A. M. & Tjandra, N. (1998). Direct structure refinement against residual dipolar couplings in the presence of rhombicity of unknown magnitude. *J. Magn. Reson.* **131**, 159-162.

79. Chou, J. J., Li, S. & Bax, A. (2000). Study of conformational rearrangement and refinement of structural homology models by the use of heteronuclear dipolar couplings. *J. Biomol. NMR,* **18**, 217-227.

80. Stein, E. G., Rice, L. M. & Brunger, A. T. (1997). Torsion-angle molecular dynamics as a new efficient tool for NMR structure calculation. *J. Magn. Reson.* **124**, 154-164.

81. Kay, L. E., Ikura, M., Tschudin, R. & Bax, A. (1989). A novel approach for sequential assignment of ^{1}H, ^{13}C and ^{15}N spectra of isotopically enriched proteins. *J. Magn. Reson.* **89**, 496-514.

82. Muhandiram, D. R. & Kay, L. E. (1994). Gradient-enhanced triple-resonance 3-dimensional NMR

experiments with improved sensitivity. *J. Magn. Reson. ser. B,* **103**, 203-216.

83. Yang, D. W., Tolman, J. R., Goto, N. K. & Kay, L. E. (1998). An HNCO-based pulse scheme for the measurement of $^{13}C^{\alpha}$-$^1H^{\alpha}$ one-bond dipolar coup-lings in ^{15}N, ^{13}C labeled proteins. *J. Biomol. NMR,* **12**, 325-332.

84. Shaka, A. J., Keeler, J., Frenkiel, T. & Freeman, R. (1983). An improved sequence for broadband decoup-ling: WALTZ-16. *J. Magn. Reson.* **52**, 335-338.

85. Kay, L. E., Ikura, M., Tschudin, R. & Bax, A. (1990). Three-dimensional triple-resonance NMR spec-troscopy of isotopically enriched proteins. *J. Magn. Reson.* **89**, 496-514.

86. Boyd, J. & Soffe, N. (1989). Selective excitation by pulse shaping combined with phase modulation. *J. Magn. Reson.* **85**, 406-413.

87. Patt, S. L. (1992). Single- and multiple-frequency-shifted laminar pulses. *J. Magn. Reson.* **96**, 94-102.

88. McCoy, M. A. & Mueller, L. (1992). Selective shaped pulse decoupling in NMR: homonuclear and ^{13}C-carbonyl decoupling. *J. Magn. Reson.* **98**, 674-679.

89. Yang, D. W. & Kay, L. E. (1999). Improved line-shape and sensitivity in the HNCO-family of triple resonance experiments. *J. Biomol. NMR,* **14**, 273-276.

90. Marion, D., Ikura, M., Tschudin, R. & Bax, A. (1989). Rapid recording of 2D NMR spectra without phase cycling. Application to the study of hydrogen exchange in proteins. *J. Magn. Reson.* **85**, 393-399.

91. Kay, L. E. (1993). Pulsed-field gradient-enhanced 3-dimensional NMR experiment for correlating $^{13}C^{\alpha/\beta}$, $^{13}C'$, and $^1H^{\alpha}$ chemical- shifts in uniformly ^{13}C labeled proteins dissolved in H_2O. *J. Am. Chem. Soc.* **115**, 2055-2057.

92. Eriksson, A. E., Baase, W. A. & Matthews, B. W. (1993). Similar hydrophobic replacements of Leu99 and Phe153 within the core of T4 lysozyme have different structural and thermodynamic conse-quences. *J. Mol. Biol.* **229**, 747-769.

93. Eriksson, A. E., Baase, W. A., Zhang, X. J., Heinz, D. W., Blaber, M., Baldwin, E. P. & Matthews, B. W. (1992). Response of a protein structure to cavity-creating mutations and its relation to the hydro-phobic effect. *Science,* **255**, 178-183.

94. Blaber, M., Zhang, X. J. & Matthews, B. W. (1993). Structural basis of amino-acid alpha-helix propen-sity. *Science,* **260**, 1637-1640.

95. Pjura, P. E., Matsumura, M., Wozniak, J. A. & Matthews, B. W. (1990). Structure of a thermostable disulfide-bridge mutant of phage T4 lysozyme shows that an engineered cross-link in a flexible region does not increase the rigidity of the folded protein. *Nature,* **345**, 86-89.

96. Rose, D. R., Phipps, J., Michniewicz, J., Birnbaum, G. I., Ahmed, F. R., Muir, A., Anderson, W. F. & Narang, S. (1988). Crystal structure of T4-lysozyme generated from synthetic coding DNA expressed in *Escherichia coli. Protein Eng.* **2**, 277-282.

97. Ottiger, M. & Bax, A. (1999). Bicelle-based liquid crystals for NMR-measurement of dipolar couplings at acidic and basic pH values. *J. Biomol. NMR,* **13**, 187-191.

Edited by P. E. Wright